Article

Current Biology

Multisensory integration of social signals by a pathway from the basal amygdala to the auditory cortex in maternal mice

Highlights

- Amygdala neurons linked to maternal behavior project to auditory cortex in mice
- These neurons respond to odor, but most consistently and robustly to pup odor
- They exhibit increased activity when the female caregiver is searching for pups
- Activating this pathway enhances responses to sound in maternally experienced mice

Authors

Alexandra C. Nowlan, Jane Choe, Hoda Tromblee, Clancy Kelahan, Karin Hellevik, Stephen D. Shea

Correspondence

sshea@cshl.edu

In brief

Nowlan et al. identify a neural pathway that enables the integration of sounds and odors as female mice engage in maternal care. They report that projection neurons from the amygdala to the auditory cortex respond to pup odor and are active while searching for lost pups. Activation of this pathway modulates auditory cortical responses to sound.

Nowlan et al., 2025, Current Biology *35*, 36–49
January 6, 2025
https://doi.org/10.1016/j.cub.2024.10.078

CellPress

CellPress

Current Biology

Article

Multisensory integration of social signals by a pathway from the basal amygdala to the auditory cortex in maternal mice

Alexandra C. Nowlan,[1] Jane Choe,[1] Hoda Tromblee,[1] Clancy Kelahan,[1] Karin Hellevik,[1] and Stephen D. Shea[1,2,3,*]
[1]Cold Spring Harbor Laboratory, 1 Bungtown Road, Cold Spring Harbor, NY 11724, USA
[2]X (formerly Twitter): @sheacshl
[3]Lead contact
*Correspondence: sshea@cshl.edu
https://doi.org/10.1016/j.cub.2024.10.078

SUMMARY

Social encounters are inherently multisensory events, yet how and where social cues of distinct sensory modalities merge and interact in the brain is poorly understood. When their pups wander away from the nest, mother mice use a combination of vocal and olfactory signals emitted by the pups to locate and retrieve them. Previous work revealed the emergence of multisensory interactions in the auditory cortex (AC) of both dams and virgins who cohabitate with pups ("surrogates"). Here, we identify a neural pathway that relays information about odors to the AC to be integrated with responses to sound. We found that a scattered population of glutamatergic neurons in the basal amygdala (BA) projects to the AC and responds to odors, including the smell of pups. These neurons exhibit increased activity when the female is searching for pups that terminates upon contact. Finally, we show that selective optogenetic activation of BA-AC neurons modulates responses to pup calls, and that this modulation switches from predominantly suppressive to predominantly excitatory after maternal experience. This supports an underappreciated role for the amygdala in directly shaping sensory representations in an experience-dependent manner. We propose that the BA-AC pathway supports integration of olfaction and audition to facilitate maternal care and speculate that it may carry valence information to the AC.

INTRODUCTION

Organisms engaged in unstructured natural behavior typically make decisions by considering all sensory data available to them. This is in sharp contrast to how most sensory neurophysiology and psychophysical research has historically been conducted. For example, during social encounters, individuals are often informed about the identity and status of conspecifics by interpreting a combination of auditory, olfactory, tactile, and/or visual cues. While the significance of all these modalities has individually been well studied, much less is known about how qualitatively distinct pieces of social information from different senses are integrated in the brain to guide behavior. Here, we examine the neural circuitry that underlies multisensory integration of odor and sound during maternal behavior in mice.

Shortly after giving birth, first-time mother mice learn to respond to ultrasonic vocalizations (USVs or "calls"), emitted by pups when they are separated from the litter, by locating them and bringing them back to the nest ("pup retrieval").[1,2] Sensory experience with pups is sufficient to motivate pup retrieval because virgin females co-housed with pups ("surrogates") also learn to retrieve without the influence of pregnancy hormones.[3–10] Consistent with the importance of USV detection for pup retrieval, activity and plasticity of the auditory cortex (AC) are implicated in accurate and efficient pup retrieval.[5–9] Audition and olfaction are jointly required because disrupting olfactory processing also interferes with retrieval.[8,11–13] Interestingly, there is evidence that separate signals related to odor and sound may merge in the AC. Delivery of pup odors to anesthetized female mice acutely modulates single neuron AC responses to a range of sounds, including USVs, but only in pup-experienced females (mothers and surrogates), not naive females.[8,9] The brain pathway by which odor information reaches the AC is unknown.

We took advantage of the ability of virgin females to learn pup retrieval to study the neural circuit that integrates odor signals in the AC. This allowed us to observe the effects of sensory experience on this pathway independent of pregnancy hormones. We report the following findings. First, we used anatomical tracing to identify a population of neurons in the basal amygdala (BA) that project into the AC. Second, we used an intersectional viral strategy to label the AC projecting BA neurons (BA-AC) with the calcium (Ca^{2+}) sensor GCaMP6s. Fiber photometry in awake, head-fixed mice revealed that BA-AC neurons respond to odor, including the smell of pups. Third, we performed fiber photometry in freely behaving mice and found that their activity is elevated during active search for pups. Finally, we optogenetically activated BA-AC neurons in anesthetized females and found that activation modulates responses to sound. This modulation switches from predominantly suppressive to predominantly excitatory after

maternal experience. Based on these observations, we propose that neurons in the BA carry odor information to the AC, where they influence auditory activity to improve pup retrieval. This contrasts with other forms of multisensory integration in the AC that emerge via inputs from primary sensory structures. Moreover, our results reveal an underappreciated role for the amygdala in directly modulating sensory representations in accordance with maternal status.

RESULTS

Olfaction is required for pup retrieval behavior in surrogate females

Nulliparous female mice that have sustained exposure to pups, e.g., via cohabitation with a mother and her litter, learn to perform efficient pup retrieval within a few days.[3,4] Previous reports regarding the influence of pup odors on auditory activity in the AC found evidence of this integration in both mothers and surrogates. Here, we took advantage of this property by performing all experiments reported here in surrogates to focus on the role of sensory experience in shaping auditory flexibility and maternal behavior.

The necessity of olfactory signals for maternal behavior in dams has already been established[8,11–13]; however, it is unknown whether surrogates share this requirement. Thus, we performed behavioral experiments to test the importance of odor cues for retrieval in surrogates. We assayed the pup retrieval performance of naive virgin females beginning prior to cohabitation with a pregnant dam and continuing throughout their surrogacy on postnatal days zero, three, and five (P0, P3, and P5, Figures 1A and 1B). Performance was quantified using a normalized measure of latency to retrieve (“latency index”; see STAR Methods).[6] Then, we used the tissue-specific toxicant methimazole (MMZ) to ablate the olfactory epithelium of these mice and measured their retrieval performance again. As expected, naive virgins exhibited poor pup retrieval (naive latency index: 0.622 ± 0.09; all values are reported as mean ± SEM unless otherwise noted). The same mice were each subsequently paired with a pregnant dam as surrogates, and they exhibited a significant decrease in retrieval latency on P3 (P3 latency index: 0.060 ± 0.01; Tukey’s multiple comparisons test; $p = 0.023$) and P5 (P5 latency index: 0.052 ± 0.01; Tukey’s multiple comparisons test; $p = 0.017$) compared with their naive performance (Figure 1C). After MMZ treatment, retrieval latency substantially increased (MMZ latency: 0.872 ± 0.08) and did not significantly differ from the latency of naive mice (Tukey’s multiple comparisons test; $p = 0.249$). This result was reflected by a similar shortening of the inter-retrieval interval across days (Figure 1D) (Mixed effects analysis; $p = 0.02$). Moreover, the percentage of pups retrieved significantly decreased from 100% for all subjects on P5 to 13.33% ± 0.08% after ablation of the main olfactory epithelium (MOE) (Figure 1E; Tukey’s multiple comparisons test, $p = 0.002$). These data are consistent with a requirement for volatile odor detection via the MOE for pup retrieval in surrogates.

Because we allowed seven days for the MMZ treatment to complete, the original pups that were familiar to the surrogate were too large and too independently mobile for further retrieval testing, and we replaced them with a younger, novel litter. We excluded the possibility that the impaired retrieval performance was simply due to the introduction of a litter of unfamiliar pups. We measured retrieval performance of the surrogates using a novel litter of pups before treatment with MMZ. The latency to retrieve novel pups and the latency to retrieve the familiar pups with which they had been co-housed did not significantly differ (Figure 1F; Wilcoxon matched-pairs signed rank test, $p = 0.625$). Comprehensive ablation of the MOE was confirmed with post-mortem histology (Figure 1G). Based on these results, we conclude that the retrieval proficiency exhibited by the surrogates was not limited to the pups with which they were co-housed. Moreover, the poor retrieval exhibited by MMZ-treated surrogates was not due to the unfamiliarity of the litter and was more likely attributable to disrupted olfactory signaling.

Projection neurons within the BA target the AC

Despite prior reports that pup odor can dramatically influence responses to auditory stimuli in the AC, the pathway by which odor signals reach the AC is unknown. We therefore used retrograde viral tracing methods to identify candidate inputs to the AC that could carry odor information and modulate auditory activity. We injected AAVrg-CAG-tdTomato (tdT) into the left AC as a retrograde neuronal tracer to label brain areas that project to the AC (Figures 2A–2D). In addition to known AC afferent structures such as the contralateral AC, the medial geniculate body of the thalamus (MGB), and the piriform cortex (Figures 2C and 2D), we observed tdT-labeled cells in both the ipsi- and contralateral basolateral and basomedial amygdala. Henceforth, we collectively refer to these amygdala subregions as the BA (Figure 2A). Neurons in the BA constitute an important component of the circuitry that governs maternal behavior. They receive multiple types of sensory input, including olfactory input,[14] and are proposed to contribute to appetitive maternal responses by conveying sensory information to the mesolimbic reward system.[15,16] In rats, inactivation of the BA selectively disrupts pup retrieval behavior while minimally affecting other maternal behaviors, like nursing,[17] suggesting that the BA participates in goal-directed aspects of maternal care. Moreover, neurons in the BA receive input from neighboring olfactory amygdala nuclei.[18] Based on these properties, we chose to focus our study on the population of BA neurons that project to the AC.

To quantify the extent of the BA-AC projection, we performed separate tracing experiments injecting AAVrg-hSyn-Cre-WPRE-hGH virus into the AC of Rosa26-stop^{flox}-H2B-GFP mice. With this strategy, Cre activated a nuclear-localized GFP in retrogradely labeled neurons, facilitating automated cell counting. Thousands of neurons (Figure 2E; 4,513 ± 1,977 cells; $n = 3$ mice) were labeled throughout the BA. To learn more about the neurochemical identity of the neurons that contribute to the BA-AC pathway, we performed additional retrograde tracing experiments in several lines of transgenic mice that express Cre in different populations of glutamatergic or GABAergic neurons (Slc17a7$^{tm1.1(cre)Hze}$/J, vesicular glutamate transporter type 1 [vGlut1]; Slc17a6$^{tm2(cre)Lowl}$/J, vGlut2; or Slc32a1$^{tm2(cre)Lowl}$/J, vesicular GABA transporter [vGAT]). Not surprisingly, injections of AAV that were Cre-independent labeled the largest number of cells in the BA-AC projection neurons (Figure 2G). Injections of AAV driving Cre-dependent expression of fluorophore, AAVrg-FLEX-tdT resulted in less extensive labeling overall, but

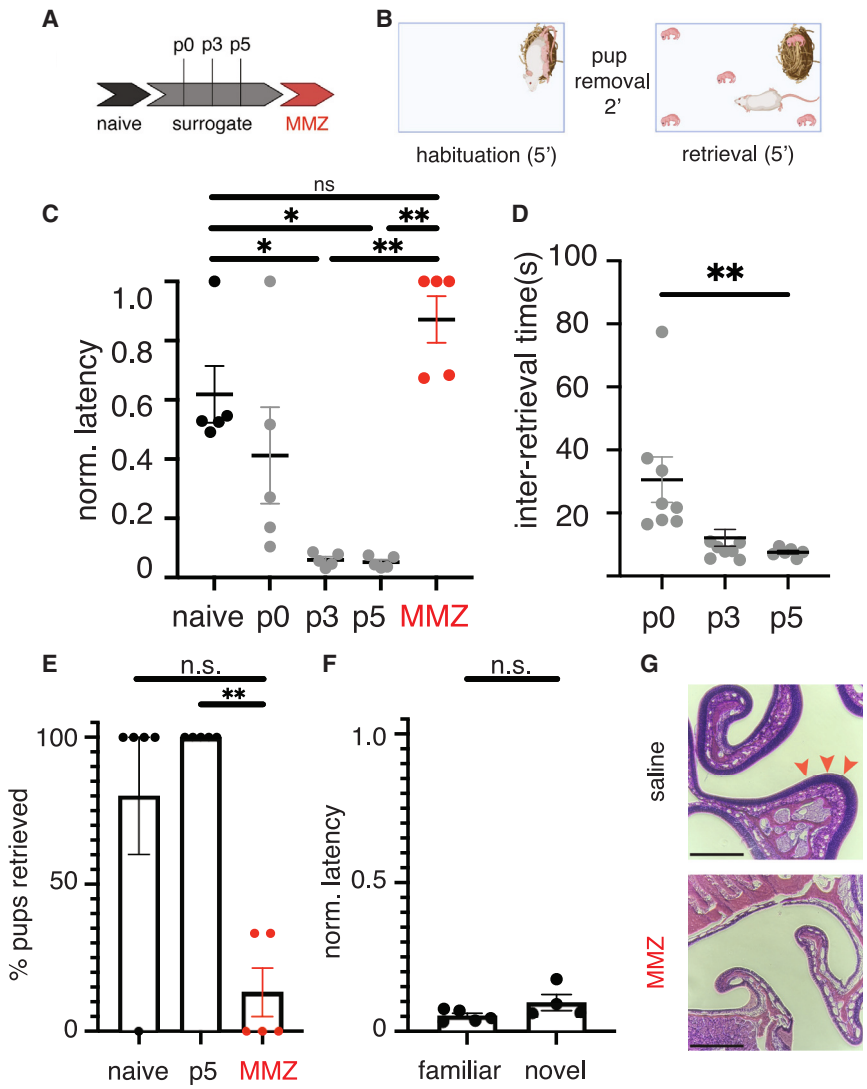

Figure 1. Olfactory signals from the main olfactory system are essential to maintain pup retrieval in surrogates

(A) Experimental timeline.

(B) Schematic of retrieval assay.

(C) Plot of latency index over time. Nulliparous female mice ($n = 5$) were assessed for pup retrieval as described prior to any exposure to pups ("naive"), on days P0, P3, and P5 relative to the birth of the pups with which they were co-housed, and again 7 days after a single IP injection of MMZ (50 mg/kg). Latency index scores (mean ± SEM) were naive: 0.622 ± 0.09, P0: 0.413 ± 0.163, P3: 0.060 ± 0.01, P5: 0.052 ± 0.01, and MMZ: 0.872 ± 0.08. Statistically significant differences between group means were determined by a repeated-measures (RM) one-way ANOVA ($F[1.95, 7.80] = 17.03$, $p = 0.0015$). All pairwise comparisons were performed using Tukey's multiple comparisons test ($^{*}p < 0.05$, $^{**}p < 0.01$). Any comparisons not depicted were not statistically significant ($p > 0.05$).

(D) Plot of inter-retrieval interval over time. This interval shortened significantly over time (mixed effects analysis, $p = 0.02$). There were insufficient trials to meaningfully quantify the inter-retrieval intervals for naive or MMZ-treated mice. Comparing P0 performance (mean ± SEM = 30.6 ± 7.2 s) to later days showed a significant reduction by p5 (7.6 ± 0.56, Dunnett's multiple comparisons test, $p = 0.009$).

(E) Bar plot comparing the percentage of pups retrieved among naive mice, surrogates on P5, and surrogates after MMZ treatment. Significant differences between time points were determined by a RM one-way ANOVA ($F[2.068, 8.727] = 8.445$, $p = 0.0097$). Pairwise comparisons were performed using Tukey's multiple comparisons test ($^{**}p < 0.01$).

(F) Plot of latency index comparing pre-MMZ performance when retrieving the familiar, co-housed pups and a novel set of pups. A pairwise comparison of these values showed no significant difference (Wilcoxon matched-pairs signed rank test, $p = 0.625$).

(G) Photomicrographs comparing representative paraffin-embedded, H&E-stained sections of the main olfactory epithelium from a mouse that received an injection of MMZ and a mouse that received a control injection of saline (scale bar, 200 μm).

See also Figures S1–S3.

only in VGlut1-Cre and VGlut2-Cre mice (Figure 2F; VGlut1-Cre: 380.3 ± 23.99 neurons, $n = 3$ mice; VGlut2-Cre: 256.3 ± 43.17 neurons, $n = 6$ mice). No retrogradely labeled neurons were found in VGAT-Cre mice ($n = 3$ mice). Based on our viral retrograde tracing experiments, we conclude that a relatively large but heterogeneous population of glutamatergic excitatory neurons in the BA project to the AC (Figure 2G).

BA-AC projection neurons respond to odors, including pup odor

To determine whether the BA-AC projection neurons were sensitive to pup-related odors, we used fiber photometry in awake head-fixed mice to measure bulk Ca^{2+} signals from BA-AC neurons in response to olfactory stimuli. We selectively labeled the BA-AC projection neurons by using the intersectional viral strategy depicted in Figure 3A (see also Figure S1). Briefly, we injected retrograde AAVrg-hSyn-Cre-WPRE-hGH into the AC and made an injection of AAV5-syn-FLEX-GCaMP6s-WPRE into the BA, thereby expressing the fluorescent Ca^{2+} sensor GCaMP6s exclusively in BA neurons that project to the AC. After 3 weeks to allow for viral expression, naive virgin females were habituated for several days to head fixation on a wheel and then presented with pseudorandomized 2 s trials of monomolecular odorants or pup odor and clean nesting material every 30 s (Figure 3B).

We observed robust, odor-evoked changes in fluorescence in response to monomolecular odors (Figures 3C–3E). Most odors in most mice elicited an abrupt increase in GCaMP6s fluorescence, although the magnitude of Ca^{2+} signals was variable depending on the individual subject and the odor presented (Figures 3D and S2). Comparing the stimulus-evoked signal to baseline for all mice, mean Ca^{2+} fluorescence showed a significant increase for each of four monomolecular odors presented

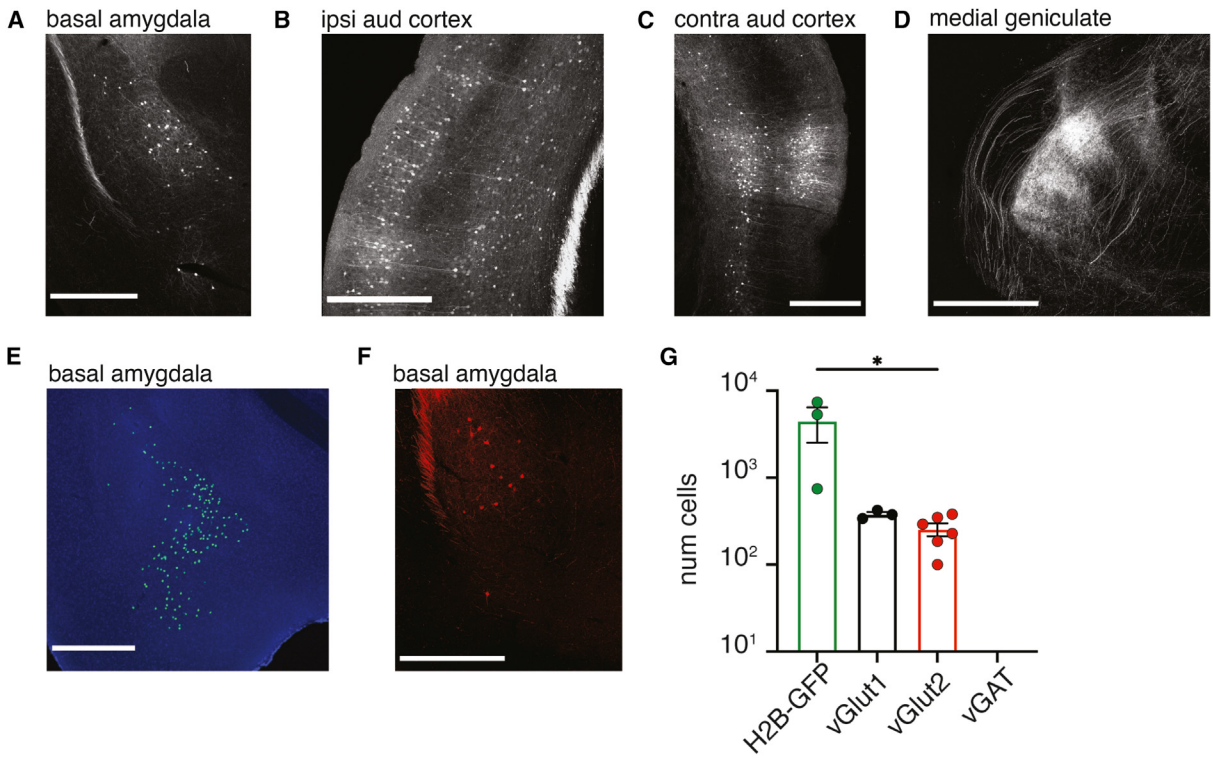

Figure 2. A subpopulation of glutamatergic neurons in the BA project to the AC

(A–D) (A) Retrograde tracing of AAVrg-CAG-tdTomato from the AC reveals cell bodies labeled within the BA, (B) throughout the ipsilateral AC, (C) contralateral AC, and (D) medial geniculate body (scale bars, 500 μm).

(E) Unrestricted retrograde tracing of AAVrg-hSyn-Cre-WPRE.hGH from the AC of a H2B-GFP mouse yields GFP positive nuclear staining for quantification of BA neurons that project to the AC (scale bars, 500 μm).

(F) Cre-restricted tracing of AAVrg-FLEX-tdTomato from the AC in vGlut1Cre mouse line (scale bars, 500 μm).

(G) Quantification of tracer positive neurons labeled by retrograde tracing from the AC in unrestricted (H2B-GFP, 4,513 ± 1,977 neurons) and Cre-restricted mouse lines (vGlut1 256.3 ± 43.17 neurons; vGlut2 380.3 ± 23.99 neurons; vGAT 0 ± 0 neurons) revealed significantly fewer tracer positive neurons in vGlut2 animals compared with H2B-GFP (Mann-Whitney test, $p = 0.0238$). We did not attempt a statistical comparison of the vGAT mice, which exhibited zero cells in all subjects, but this is consistent with BA-AC neurons being a glutamatergic population. Each point represents the counts from an individual animal.

(Figure 3E). Filled points in Figures 3E and 3F denote individual mice that exhibited significant responses to a given odor, as assessed with a bootstrap procedure (see STAR Methods). We confirmed that the responses to these stimuli were mediated by the main olfactory system by ablating the MOE with MMZ. After ablation, we no longer observed significant responses to any of the monomolecular odors (Figure 3F).

In addition to the arbitrary, non-social odors, we presented pup odor by collecting the headspace of a glass jar containing several pups (age 2–4 days) and directing the stream of odorized air onto the nose of a head-fixed, fiber-implanted mouse. In virgin females without maternal experience ("naive"), we observed a clear increase in Ca^{2+} signal in response to pup odor that had a similar temporal structure to the responses to non-social odors (Figures 4A and 4B). Pup odor-evoked responses persisted throughout the surrogacy experience (Figures 4B, 4C, and 4E). As seen with other odors, this response was abolished after MMZ treatment (Figures 4C and 4D). No odor-evoked changes in fluorescence were observed in control animals injected to express GFP in BA-AC neurons instead of GCaMP6s (3A; paired t test comparing Z-dFF at baseline (2 s) to after odor delivery (3 s), $p > 0.05$, Figure S3B; Wilcoxon signed rank test, $p > 0.05$), verifying that the fluctuations we measured in response to odors reflect neural activity and not movement or other artifacts. Based on the above data, we conclude that the BA-AC projection neurons respond to pup odor and therefore constitute a likely candidate pathway for odor information to access the AC.

The property of responding to pup odor was consistent among all mice when recording from BA-AC neurons. In addition to neurons that project to the AC, BA contains separate neurons that project to either nucleus accumbens (NAcc), the ventral hippocampus, or other targets. To assess whether response to volatile odors from pups is a shared property among all neurons in BA, we performed head-fixed recordings from BA neurons that project to the NAcc (BA-NAcc) while presenting clean nesting material, chow, and pup odor. Our viral strategy for labeling BA-NAcc neurons was very similar to the strategy we used to label the BA-AC (Figure 3A). In this case, we expressed GCaMP6s in BA-NAcc by injecting retrograde AAVrg-hSyn-Cre-WPRE-hGH into NAcc and AAV5-syn-FLEX-GCaMP6s-WPRE into the BA (Figure S4A).

After ~3 weeks to allow for expression, nulliparous adult female mice ($n = 6$) were delivered a 2 s trial of either pup odor, chow, or clean nesting material in pseudorandomized order every 30 s (Figures S4B and S4C). All mice consistently exhibited

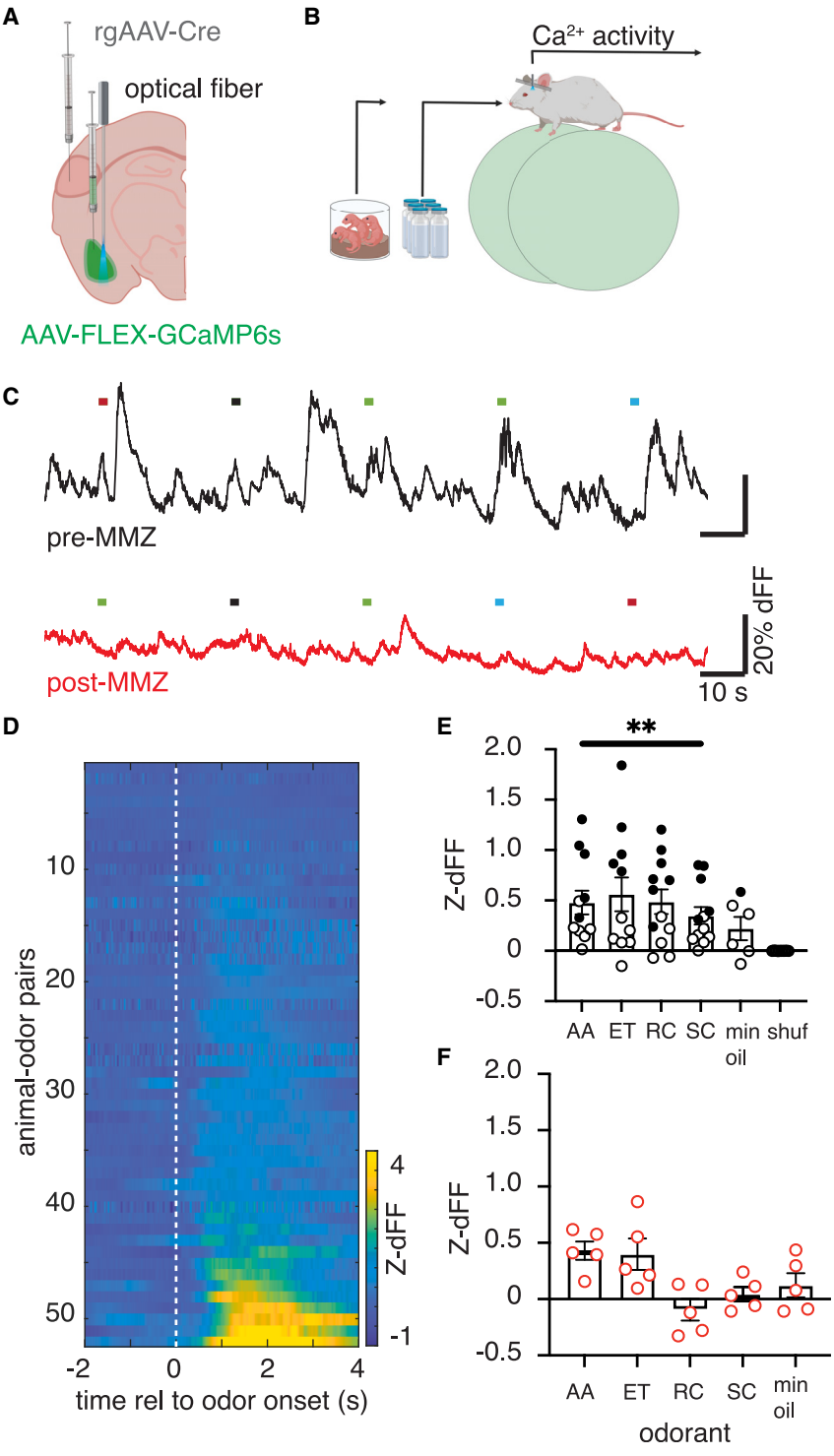

Figure 3. BA-AC projection neurons exhibit increased Ca^{2+} activity in response to olfactory stimuli

(A) Schematic of our intersectional viral strategy for selectively labeling BA-AC projection neurons with GCaMP6s and recording ongoing Ca^{2+} activity.

(B) Schematic of head-fixed recording of Ca^{2+} activity during presentation of monomolecular odorants or pup odor.

(C) Raw dFF traces from one animal during the presentation of monomolecular odorants before MMZ treatment (top, black trace) and after MMZ treatment (bottom, red trace). Dashed lines are color coded by odor stimulus. Black dashes are mineral oil controls.

(D) Heatplot of mean responses to all odors by all mice. Each row in the plot represents the mean response over multiple trials to one odor in one mouse (odor-mouse pair), expressed as a *Z* score (Z-dFF), according to the color bar. Rows are ordered by the magnitude of each response.

(E) Quantification of the increased Ca^{2+} signal during odor presentation. (top): responses to all odors were observed among recorded subjects (n = 13 mice). Filled circles indicate mean responses that were outside the center 95% of a dummy distribution generated with a bootstrap procedure using data from the same mouse (see STAR Methods). For each odor, the responses of all mice were compared with a mean response of 0: amyl-acetate (AA: 0.4788 ± 0.1180), S-carvone (SC, 0.3478 ± 0.0859), ethyl tiglate (ET: 0.5605 ± 0.186), R-carvone (RC: 0.4868 ± 0.1220), linalool (LN: 0.6282 ± 0.2049), mineral oil (min oil, 0.2215 ± 0.1159), and shuffled data (shuf, −0.0002 ± 0.0005). Wilcoxon signed rank test, $^{**}p < 0.01$ (bottom).

(F) No significant odor responses were observed to any odor, at either the population or individual mouse level following treatment with MMZ (AA: 0.3679 ± 0.1182; ET: 0.2452 ± 0.1338; RC: −0.1408 ± 1090; SC: −0.0559 ± 0.1402, min oil: 0.1916 ± 0.0631, n = 5).

See also Figures S1–S3.

no response to pups or the blank (empty vial) stimulus, and several mice exhibited responses to nest material and chow, but when comparing mean odor-evoked responses of all mice to each odor with zero, only responses to chow achieved statistical significance (n = 6, one sample t test; $p < 0.05$). These results demonstrate that information regarding pup odors is shared with AC, but not all BA targets.

BA-AC neurons are active during pup seeking

Having discovered that BA-AC neurons were sensitive to pup odor, we next asked how they may participate in free interactions with pups, including retrieval. To do this, we recorded Ca^{2+} activity from BA-AC neurons in freely behaving females daily as they performed pup retrieval from the naive state through surrogacy. Based on the results of the head-fixed experiments, we hypothesized that we would observe odor-evoked responses in the BA-AC neurons when a naive female engaged with pups by picking them up or sniffing them during the retrieval behavior.

Surprisingly, by aligning the fluorescent traces to the mouse's behavior, we observed that while searching for pups (defined here as the time between egress from the nest and either contact with a pup or returning to the nest), Ca^{2+} signals were elevated

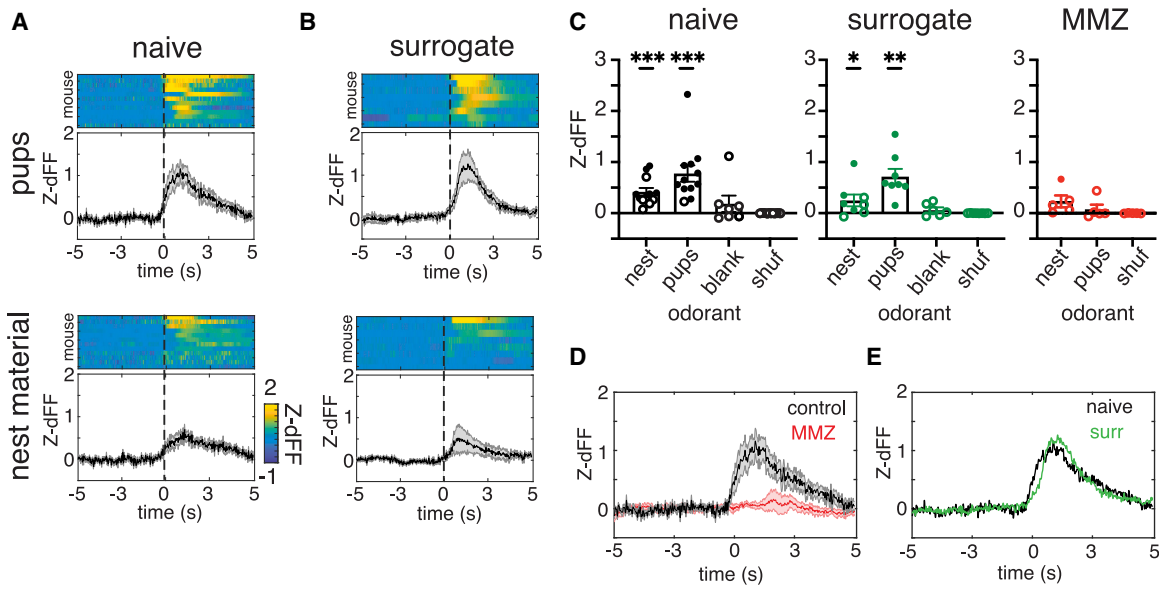

Figure 4. Pup-odor-evoked activity is maintained across surrogacy

(A and B) (A) Normalized evoked responses to pups and clean nest material in naive and (B) surrogate animals. Heatmaps were sorted by decreasing strength of response (top) to demonstrate the variability of average odor-evoked activity across animals with SEM indicated by shaded area (bottom). Color scale applies to all heatmap plots.

(C) Quantification of the Z-dFF signal during odor presentation in naive animals (nest: 0.416 ± 0.078, pups: 0.776 ± 0.16, blank: 0.184 ± 0.16, and shuffled data: −0.0005 ± 0.0011, n = 7–12, closed circles indicate mean responses that exceeded a 95% cutoff of bootstrapped data), surrogates (nest: 0.249 ± 0.11, pups: 0.716 ± 0.15, blank: 0.066 ± 0.050, and shuffled data: −0.0001 ±0.0001, n = 6–8), and after MMZ treatment (nest: 0.230 ± 0.12, pups: 0.077 ± 0.091, and shuffled data: −0.0001 ± 0.0025, n = 5). Each point represents a single animal. Bars indicate mean ± SEM Wilcoxon signed rank test.

(D and E) (D) Average pup-odor evoked activity comparing response from naive animals (black trace, n = 12) and MMZ-treated animals (red trace, n = 5), and (E) naive (black trace, n = 12) versus surrogate animals (green trace, n = 8).

See also Figures S1–S4.

(Figure 5A). For a more systematic analysis, we segmented pup retrieval into four behavioral events: pup retrieval, pup sniffing, air sniffing, and search. When GCaMP6s traces were aligned to each phase of retrieval, BA-AC neurons only showed a significant increase in activity as the females (n = 10 mice) searched the cage for a pup (Figure 5D; Wilcoxon signed rank test, p = 0.027), not when they made contact to retrieve or engaged with a pup physically by sniffing it. In fact, the fluorescent signal dropped significantly as soon as contact with a pup was made for retrieval (Figures 5B–5D, Wilcoxon signed rank test, p = 0.004) or investigation (Figure 5D; Wilcoxon signed rank test, p = 0.010). In Figure 5B, the variability seen among the individual trials and the ramping appearance leading up to contact are due to the fact that animals can spend very different amounts of time on individual search bouts. These results suggest that the BA-AC circuit is primarily active during exploratory and/or goal-directed aspects of maternal behavior.

This relationship between neural activity and behavior was not explained by a simple correlation between activity and movement or locomotion. We used the machine learning-based markerless pose estimation tool SLEAP[19] to track the mouse's head position during the majority of behavior trials contributing to the data in Figure 5. For 2/9 mice, the videos were too dark to be correctly labeled on more than a few percent of frames. For the remaining seven mice, when we correlate neural activity with speed (directionless velocity), we find that they are only (positively) correlated specifically during the part of the video where the female is actively retrieving pups. Activity and speed are unrelated when considering the entire experiment or only the post-retrieval time period.

Optogenetic activation of BA-AC neurons bidirectionally modulates AC activity

Acutely presenting pup odor modifies auditory responses in the AC of female mice with maternal experience. Having established that the BA-AC projection neurons are responsive to pup odor and are active while the female searches for pups, we therefore hypothesized that selective optogenetic activation of the BA-AC pathway may modulate auditory responses in AC. We tested this hypothesis using an intersectional viral strategy to selectively label the BA-AC projection neurons with either the excitatory opsin, Channelrhodopsin-2 (ChR2), or GFP as a control (Figures 6A and S5). Due to the fact that the retrograde Cre viral construct does not include a fluorophore, only the BA-AC neurons were labeled. Therefore, we were able to observe segments of labeled BA-AC throughout the AC (Figure S5). After several weeks to allow for stable viral expression, mice in both groups were used for acutely anesthetized extracellular recording experiments. Auditory cortical neurons were recorded with the "loose patch" technique[5,20] while presenting a set of tones and pup vocalizations (calls) in pseudorandom order (see STAR Methods). On 50% of trials, BA-AC axon terminals labeled with ChR2 were activated by directing blue light (473 nm) onto the cortical surface (Figure 6B). To examine the effect of maternal

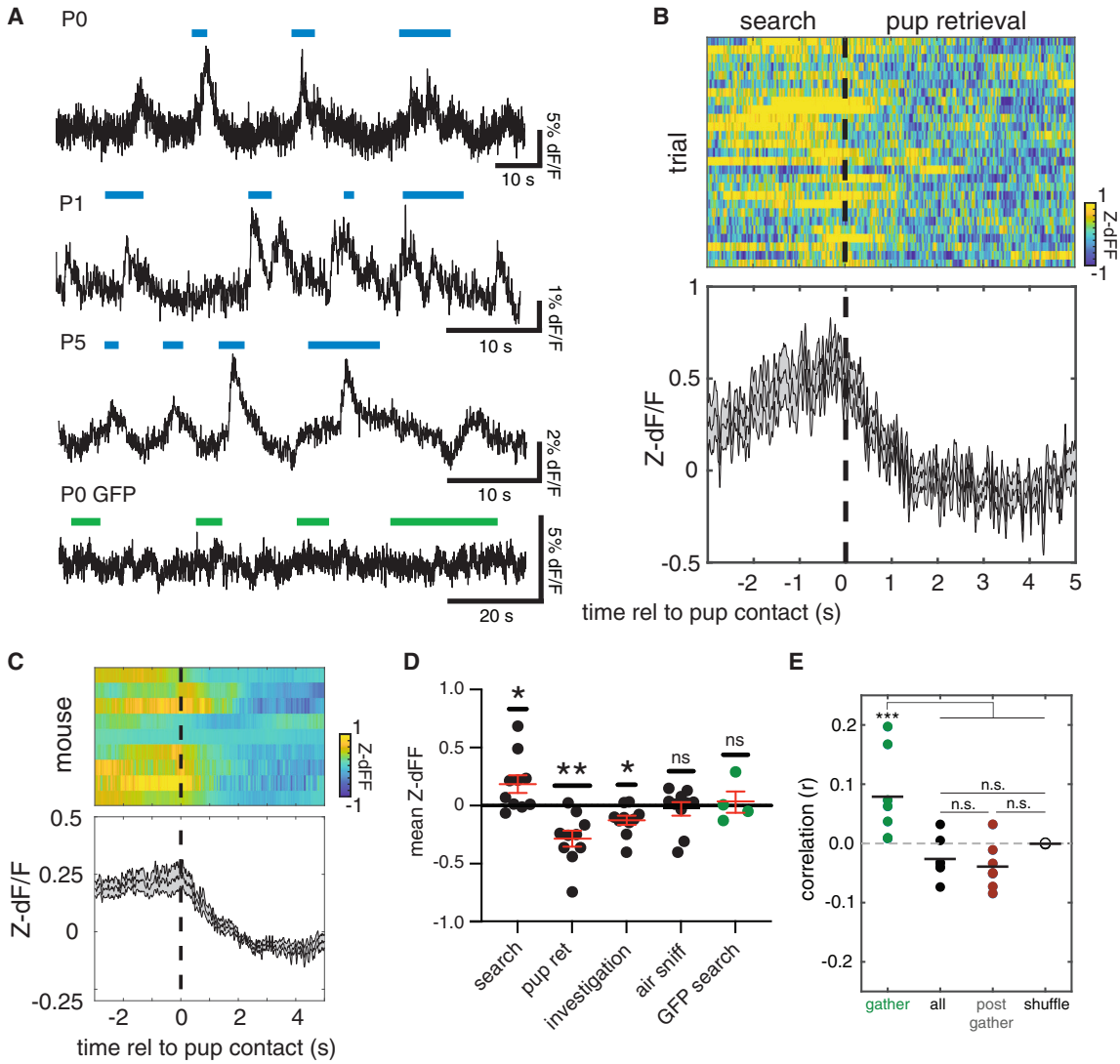

Figure 5. BA-AC neurons show elevated activity during pup search that terminates with pup contact

(A) Example traces of dFF during several episodes of searching for pups. Each trace is taken from a different mouse on a different postnatal day (shown to the upper left of each trace). The colored bars above each trace denote time spent searching for a pup, beginning at the time the female exits the nest and ending at the time she contacts a pup. The blue bars are above traces taken from mice expressing GCaMP6s in BA-AC neurons. The trace with the green bars above it was taken from a mouse that was expressing GFP in BA-AC neurons.

(B) Average data across all retrieval trials from one mouse aligned to the end of the search period. The upper panel is a heat map of Z-dFF for 27 retrieval events taken from P0, P1, P3, and P5. Each row depicts one retrieval event aligned to the end of the search period when the mouse contacts the pup (vertical dashed line). Color is mapped to Z-dFF according to the color bar on the lower right. The lower panel is a plot of mean Z-dFF for all trials. The shaded area around the trace denotes the SEM of the response. Note the abrupt decrease in activity as the female encounters the pup.

(C) Plot summarizing the average response to pup contact in all mice. The upper panel is a heatmap of the average response to a search that terminates in an encounter with a pup across all trials for all mice ($n = 9$). Each row is the mean response to pup contact (vertical dashed line) for one mouse, calculated as in (B). Color is mapped to Z-dFF according to the color bar on the lower right. The lower panel is a plot of mean Z-dFF for all mice. The shaded area around the trace denotes the SEM of the response.

(D) Plot of the mean change in fluorescence associated with several events (search, pup contact, investigation, and air sniff) across all mice. Each point denotes the mean response of one mouse, defined as the difference between the mean fluorescence during the first 3 s after each event and the mean value during the immediately preceding 3 s. Mean activity during search (0.1863 ± 0.076 Z-dFF), after pup contact (−0.284 ± 0.068 Z-dFF), and during investigation (−0.126 ± 0.040 Z-dFF) were significantly different from 0 ($n = 10$ mice; Wilcoxon signed rank test, $^{*}p < 0.05$, $^{**}p < 0.01$). No significant change in fluorescence was detected when the mouse sniffed the air ($n = 10$ mice; −0.028 ± 0.057 Z-dFF, Wilcoxon signed rank test, $p = 0.695$) or in mice that expressed activity-independent GFP in the BA ($n = 4$; 0.030 ± 0.092 Z-dFF, Wilcoxon signed rank test, $p > 0.999$).

(E) Plot of the mean correlation coefficients (r) between neuronal signal and locomotion as measured by the mouse's speed (directionless velocity). Correlations were computed separately for the time up until retrieval is complete (green) and the remaining time (red). Black dots show the mean correlation coefficients computed over the whole trial, and white dots are the values reached after shuffling time bins.

See also Figure S1.

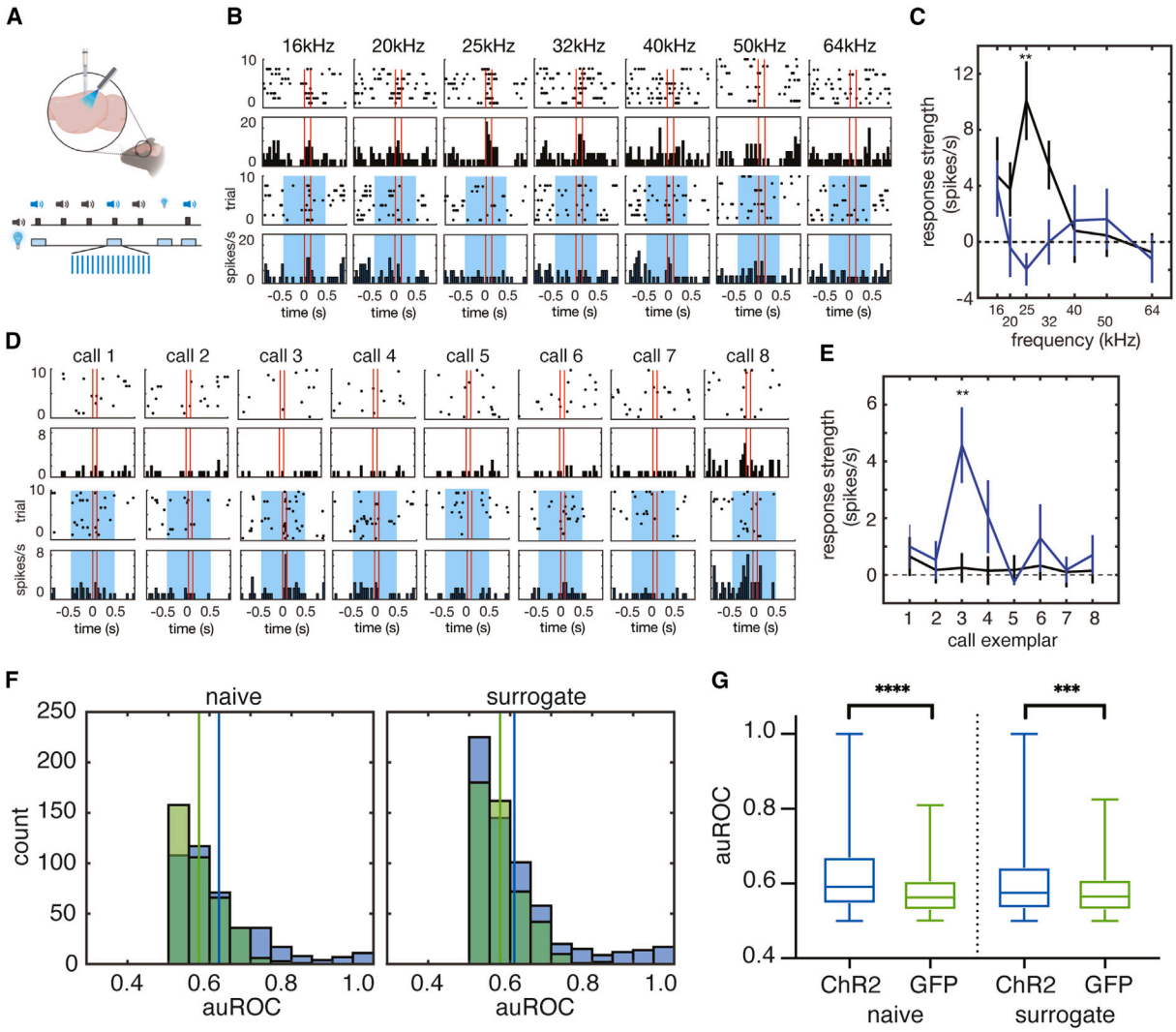

Figure 6. Optogenetic activation of the BA-AC pathway elicits widespread and bidirectional modulation of auditory responses in the auditory cortex

(A) Schematic of the experimental design. The same intersectional strategy for labeling BA-AC neurons with GCaMP6s (Figure 3A) was used to express ChR2 in the same neurons. The retrograde virus AAVrg-hSyn-Cre-WPRE-hGH was injected into the AC, and at the same time, the Cre-dependent AAV9-CAGS-FLEX-ChR2-tdT-WPRE-SV40 was injected into the BA. Mice were acutely anesthetized for electrophysiology recordings and presented with auditory stimuli, including synthesized pure tones and previously recorded pup calls. Stimuli were presented in a pseudorandom order, and 50% of trials for each stimulus were accompanied by a train of 473 nm light pulses (20 Hz) directed at the cortical surface to activate BA-AC terminals.

(B) Plots comparing responses of an auditory cortical neuron to logarithmically spaced pure tones when presented during light activation of BA-AC and when presented alone. Data are from a naive female. Each stimulus is associated with a raster plot and peristimulus time histogram (bin size = 50 ms) from control trials (top row) and from light activation trials (bottom row with blue shading). The blue shading denotes the duration of the light train relative to the tone. Note that responses to the 25 kHz tone are significantly weaker when BA-AC terminals were activated by light (n = 8 trials; comparison of trials with and without light, unpaired t test with Bonferroni correction, $^{**}p < 0.01$).

(C) Line plot of data from (B) comparing the mean baseline-subtracted firing rate evoked by each tone on control trials (black) and on light trials (blue) ($^{**}p < 0.01$). Vertical lines denote SEM.

(D) Plots comparing responses of a different auditory cortical neuron to 8 different pup call exemplars when presented during light activation of BA-AC and when presented alone. Data are from a surrogate female. Panels are organized as in (B).

(E) Line plot of data from (D) comparing the mean baseline-subtracted firing rate evoked by each call on control trials (black) and on light trials (blue). Note that in this case, responses to call 3 are significantly stronger when BA-AC terminals were activated by light (n = 8 trials; comparison of trials with and without light, unpaired t test with Bonferroni correction, $^{**}p < 0.01$).

(F) Distribution of auROC values for each cell-stimulus pair from ChR2-injected animals (blue) and GFP controls (green) separated by pup experience (naive, left; surrogate, right). The mean value of each distribution is marked by the vertical line of the corresponding color.

(G) Box plots of the data in (F) demonstrate that ChR2 expressing animals exhibit significantly greater discriminability between light-on and light-off trials for both naive virgins (ChR2: n = 415 cell-stimulus pairs, 0.623 ± 0.005; GFP: n = 376 cell-stimulus pairs, 0.574 ± 0.003, Mann-Whitney U test, $p < 0.0001$) and surrogates (ChR2: n = 616 cell-stimulus pairs, 0.610 ± 0.005; and GFP: n = 469 cell-stimulus pairs; 0.576 ± 0.003, Mann-Whitney U test $p = 0.0005$).

See also Figures S5–S7.

experience, recordings were performed in either naive virgins or surrogate mothers.

We recorded 83 neurons from 17 ChR2-injected mice (34 from 7 naive mice and 49 from 10 surrogates) and 72 units from 15 GFP-injected mice (33 from 7 naive and 39 from 8 surrogates). All neurons exhibited stimulus-specific activity, and in ChR2-expressing mice, responses to some or all stimuli were modified by optogenetic activation. For example, on trials without light stimulation, the neuron depicted in Figures 6B and 6C showed significant increases in firing to 16, 20, 25, and 32 kHz tones. However, in trials with light activation of the BA-AC terminals, responses to several tones were abolished (Figures 6B, lower and 6C, blue trace). In some neurons, stimuli that elicited no response on trials without optogenetic activation actually did evoke a significant response on trials with light (Figures 6D and 6E).

We quantified the magnitude and the prevalence of light modulation for all neurons and stimuli by performing a receiver operator characteristic (ROC) analysis for each cell-stimulus pair (see STAR Methods). In this analysis, the area under the ROC curve (auROC) can be used as a measure of the discriminability between light-on versus light-off trials. We found that in naive virgins, the auROC values for units recorded from ChR2 animals were significantly greater than those observed in GFP controls (Figures 6F and 6G; ChR2: 0.62 ± 0.01; GFP: 0.574 ± 0.00, Mann-Whitney U test, $p < 0.0001$). The same was true in surrogates (Figures 6F and 6G, ChR2: 0.61 ± 0.01; GFP: 0.58 ± 0.00, Mann-Whitney U test $p = 0.0005$). Because in this analysis the responses of cells to different stimuli are potentially not independent, we performed a hierarchical bootstrap analysis[21] (and see STAR Methods) for analyzing multilevel data. This analysis showed that the bootstrap distributions obtained by resampling each group were significantly different (joint probability distribution, $p < 0.01$). Therefore, the modulation of auditory responses was due to optogenetic activation and not light itself.

The direction of modulation was not accounted for in the above analysis, but it varied by neuron and stimulus. We observed examples of both optogenetic enhancement *and* suppression of auditory response strength in naive females (Figures 6C and 6E) and surrogates (Figure S6). However, a comparison of the effect of optogenetic activation of the BA-AC pathway revealed that maternal experience flipped the balance from predominantly suppression in naive females (Figure 7A) to predominantly enhancement in surrogates (Figure 7B).

To determine whether stimulus frequency might influence this categorical outcome, we used Fisher's exact test to compare the number of units enhanced and suppressed by optogenetic stimulation from ChR2-injected animals versus GFP controls. For the majority of tones presented, the effect of optogenetic activation on AC responses to sound was independent of tone frequency (Figure S7A). The only exception was naive responses to 32 kHz tones (Fisher's exact test, $p = 0.02$). Similarly, the effect of activation of the BA-AC pathway was independent of the call exemplar presented, with the exception of surrogate responses to call exemplar 5 (Figure S7B, Fisher's exact test, $p = 0.0003$).

To quantify the relative preponderance of optogenetic enhancement versus suppression observed in surrogates, we calculated a modulation index (see STAR Methods) to measure the change in response strength between light-off and light-on trials. We observed significant differences in modulation index between the naive and surrogate animals for both tone stimuli (Figure 7C; naive: $n = 226$ cell-stimulus pairs, −0.19 ± 0.04; surrogate: $n = 291$ cell-stimulus pairs, 0.031 ± 0.03; Mann-Whitney U test, $p < 0.0001$) and USVs (Figure 7C; naive: $n = 175$ cell-stimulus pairs, −0.110 ± 0.042, surrogate: $n = 274$ cell-stimulus pairs, 0.055 ± 0.032; Mann-Whitney U test, $p = 0.0006$). There was no difference in the modulation index between naive and surrogate GFP control mice for either tone or USV stimuli (Figure 7D; Mann-Whitney U test, $p > 0.05$). Similar to what we observed in the number of enhanced units, the distribution of modulation indices was independent of stimulus identity (Figures S7C and S7D; naive, 2-way ANOVA, $p > 0.05$, $n = 34$ units, 7 mice; surrogates, 2-way ANOVA, $p > 0.05$, $n = 46$ units, 10 mice).

In some cases, we observed a change in firing rate on light-only trials, during which no auditory stimulus was played (e.g., Figure 7E). While only some cells exhibited a change in firing on light-only trials, considering all cells from ChR2-expressing mice, we found that light-only responses were significantly more positive in surrogates as compared with the effect of optogenetic BA-AC activation in naive mice (Figure 7F; naive: $n = 34$ neurons, −0.09 ± 0.08; surrogates: $n = 49$ neurons, 0.24 ± 0.10, Mann-Whitney U test, $p = 0.025$). Again, we discovered a significant experience-dependent bias in the strength of the light-only response. In naive animals, ongoing activity was suppressed by activation of the BA-AC pathway, while in surrogates it was enhanced.

DISCUSSION

Like most social encounters, interactions between rodent pups and their parents are multisensory. They include somatosensory components and, most relevant to this work, auditory and olfactory components. The importance of pup vocalizations for eliciting retrieval is clear from several observations. First, dams will phonotax toward playback of natural USVs and synthetic USVs within the appropriate high-frequency range.[22] Second, pups that are congenitally mute are largely ignored by their mothers, even when they are separated from the nest.[23] Third, many studies have shown that initial maternal experience in both dams and virgin surrogates is correlated with plasticity in auditory responses in the AC.[5–9] Finally, in our prior work on the impairment of maternal behavior in a mouse model of Rett syndrome (*Mecp2*^{het}), we showed that knocking out *Mecp2* only in the AC post-development was sufficient to substantially impair retrieval performance.[6,24]

Although less well studied, olfactory cues from the pups are also acknowledged to be essential for pup retrieval. For example, interfering with a mother's ability to detect volatile pup odors, either by genetically inactivating crucial components of olfactory signaling or by washing the pups to remove their odor, significantly diminishes retrieval performance.[8,11–13] Notably, here we confirmed and extended this finding to include virgin surrogates that had already established retrieval proficiency. By using the tissue-specific toxicant MMZ to ablate the MOE, we demonstrated that they almost completely lost the ability to gather pups. MMZ is also used to reduce thyrotropin-releasing hormone (TRH) levels. TRH signaling deficiency can interact with impairments in the oxytocin system, and the available data suggest that, in isolation, TRH receptor loss affects

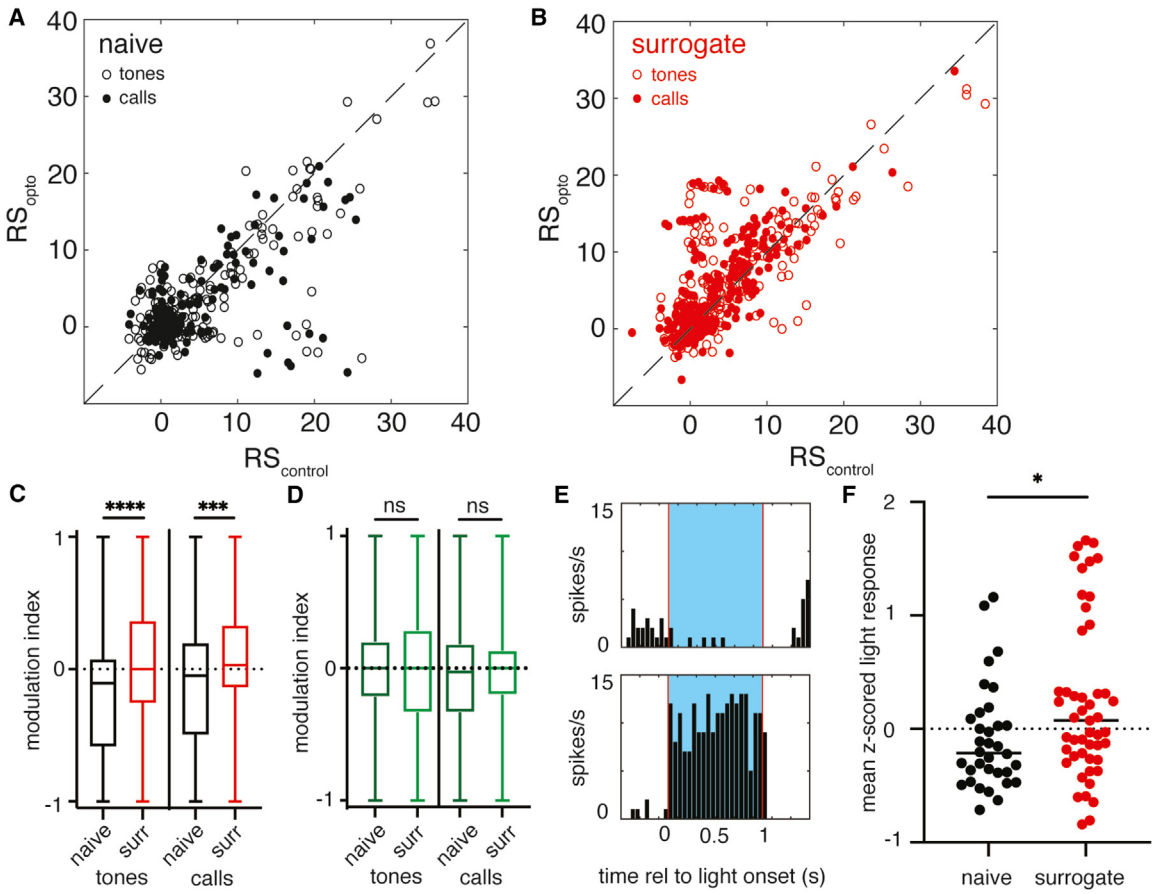

Figure 7. The effects of BA-AC activation on AC neurons are experience dependent

(A) Scatterplot of response strength (RS) comparing control trials versus light activation trials for all cell-stimulus pairs in naive mice expressing ChR2 in BA-AC neurons. Tone stimuli are plotted as open circles, and call stimuli are plotted as filled circles.

(B) Scatterplot of response strength (RS) comparing control trials versus light activation trials for all cell-stimulus pairs in surrogate mice expressing ChR2 in BA-AC neurons. Tone stimuli are plotted as open circles, and call stimuli are plotted as filled circles.

(C) Box plot of modulation index comparing modulation of tone responses in naives (black) and surrogates (red) expressing ChR2 in BA-AC (naive: $n = 226$ cell-stimulus pairs, -0.185 ± 0.037; surrogates: $n = 291$ cell-stimulus pairs, 0.031 ± 0.034; Mann-Whitney U test, $p < 0.0001$) (left side). On the right side, the box plot compares modulation of USV call responses in naives (black) and surrogates (red) (naive: $n = 175$ cell-stimulus pairs, -0.110 ± 0.042, surrogate: $n = 274$ cell-stimulus pairs, 0.055 ± 0.032; Mann-Whitney U test, $p = 0.0006$ Mann-Whitney U test).

(D) Box plot of modulation index comparing modulation of tone responses in naives (dark green) and surrogates (light green) expressing GFP in BA-AC (naive: $n = 213$ cell-stimulus pairs, -0.027 ± 0.031; surrogates: $n = 223$ cell-stimulus pairs, -0.005 ± 0.038; Mann-Whitney U test, $p = 0.453$) (left side). On the right side, the boxplot compares modulation of USV call responses in naives (black) and surrogates (red) (naive: $n = 153$ cell-stimulus pairs, -0.078 ± 0.040; surrogate: $n = 206$ cell-stimulus pairs, -0.020 ± 0.030; Mann-Whitney U test, $p = 0.204$).

(E) Example responses to light-only trials for naive and surrogate mice. The top panel shows a peristimulus time histogram (bin size = 50 ms) of the mean firing rate of an AC neuron in a naive female during 20 trials of light stimulation accompanied by silence. The bottom panel shows a peristimulus time histogram (bin size = 50 ms) of the mean firing rate of an AC neuron in a surrogate female during 20 trials of light stimulation accompanied by silence.

(F) Swarm plot comparing the mean response to light-only trials for all neurons in ChR2-expressing mice. (naive : $n = 34$, -0.091 ± 0.089; surrogates: $n = 49$, 0.237 ± 0.101; Mann-Whitney U, $p = 0.0248$).

See also Figures S5 and S7.

parenting quality weakly if at all.[25] Still, we cannot rule it out. Nevertheless, the most straightforward interpretation is that MMZ works through its ablation of the MOE. This raises several possibilities for the role olfactory cues play in maternal retrieval behavior: they may help guide the female to the location of the pup, they may influence the perception of USVs, and/or they may trigger maternal experience-induced plasticity in the AC.

Despite the shared importance of USVs and pup odor for maternal care, relatively little is known about the circuits that coordinate audition and olfaction during maternal behavior. Previous work by Cohen and colleagues[8,9] showed that the odor of pups directly interacts with AC responses to sounds, including USVs. Importantly, this interaction was only observed in mothers or surrogates with maternal experience. However, the circuit by which the pup odor accessed the AC was not identified.

Here, we attempted to identify a specific neural pathway that could integrate the influence of odor with sensory representations of USVs in the AC. We began by injecting viral tracers

into the AC to reveal candidate inputs. We identified the BA as a region that could carry information regarding odors due to its connections to olfactory areas of the amygdala.[18] We also observed sparse labeling of neurons in the piriform (olfactory) cortex. Nevertheless, in light of prior studies linking the BA with maternal behavior (see below), we instead chose to focus on its projection to the AC.

We made the following observations regarding the BA-AC pathway: first, we identified the BA neurons that project to the AC as likely predominantly glutamatergic, and this population shows signs of diversity, based on the apparent mixed expression of VGlut isoforms. We do not know the significance of this diversity, but our results show starkly that the pathway is primarily, if not exclusively, glutamatergic. Second, with fiber photometric recordings exclusively from BA neurons that project to the AC, we demonstrated that these neurons robustly respond to pup odor and other odors more broadly. Third, we found that BA-AC neurons are active in freely behaving surrogates, particularly while the mouse is searching for pups, and rapidly become less active when she contacts them. Fourth, we found that optogenetic activation of the terminals of BA-AC projections changed the response of AC neurons to sound, sometimes dramatically. Finally, in naive virgins, activation predominantly led to inhibition of auditory responses, while in surrogate mice, activation predominantly led to excitation. We conclude that a glutamatergic projection from the BA regulates auditory cortical activity in an experience-dependent manner during pup interactions, in part driven by odors.

Implications for the AC

The pathway from the BA to the AC has not been widely studied. Responses to sound in AC are modulated by emotionally charged stimuli,[26–31] but evidence that the modulation comes directly from the amygdala is sparse. We hypothesize that the BA-AC pathway is a potential conduit for information about valence to reach AC. This may have important short-term and long-term consequences for how the AC responds to behaviorally significant sounds. Cohen et al.[8] reported a significant influence of pup odor on responses to a variety of sounds. However, the design of their experiments precluded a trial-by-trial assessment of this influence. Instead, they recorded responses in alternating blocks lasting tens of minutes, either with or without pup odor. We used an optogenetic approach that enabled precise optical control of BA inputs on the temporal scale of individual sounds. These experiments demonstrate that the BA projection is capable of rapidly modulating auditory responses. On the other hand, optogenetic activation exhibited long-term experience dependence. Modulation of the AC by pup odor was only observed in mice with pup experience, not naive virgin mice. In our experiments, pup odor responses in the BA (at least in head-fixed surrogates) were evident prior to pup exposure and continued at least until P5. Moreover, after pup exposure, the effects of activating BA inputs shifted from being predominantly inhibitory to predominantly excitatory. This strongly implies that the intrinsic circuitry of the AC and/or how it is accessed by BA afferents undergo long-term plasticity.[30,32] It also raises the possibility that pup odor may indeed be an important trigger for AC plasticity that has been commonly observed following maternal experience.

Our results resemble sensory learning seen in several systems in which circuits in a primary sensory region show enduring changes to responses after they have been accompanied by a neuromodulatory or other signal that marks the occasion as behaviorally significant. For example, the release of noradrenaline stimulated by a social encounter or mating event unleashes plasticity in the main and accessory olfactory bulbs that permanently alter the circuitry and change its response to odor stimuli or input.[33,34] A similar change occurs in the AC when sounds are repetitively paired with activation of cholinergic afferents from nucleus basalis.[35–37]

Behavioral function of BA

The BA is activated during maternal behavior and in response to multisensory pup stimuli. Presenting mothers with either a hypothermic pup or the combination of pup odors and USVs results in significantly elevated *c-fos* expression in the BA relative to controls presented with no stimulus.[14] In that study, the synaptic targets of pup-responsive BA neurons were not identified, but the BA has been suggested to influence appetitive maternal behaviors (e.g., retrieval) through its projections to the NAcc and ventral pallidum.[38,39] Our results here argue that, in addition to regulating reward circuitry, the BA might contribute to goal-directed maternal behaviors in a previously unappreciated manner by regulating the auditory processing of USVs. Interestingly, neurons in one of these other output pathways (BA-NAcc) showed no response to pup odors, raising the possibility of complexity in how different information regarding pup encounters may be private or shared with different BA targets.

One intriguing aspect of our data is that in addition to being activated by pup odor, responses in the BA-AC pathway are also evoked by arbitrary, monomolecular odorants, albeit less consistently. This may indicate that responses to pup odors in BA-AC neurons are embedded in a broader functional context. This may represent a salience signal rather than simply a sensory response. One potentially fruitful area of future work would be to assess the relationship between BA response to cues associated with reward, punishment, and salience and responses to pups. Are responses to novel conditioned cues shared with responses to pup odor at the level of single neurons, and what are the valences of those responses? Another important question is whether either type of response is sensitive to learning. If they are, that might yield clues to the ultimate function of the pathway. Sustained responses over time could point to BA-AC neuron activity as a driver of retrieval, whereas transient responses early in task experience that later recede may suggest that it is a permissive signal for learning based on emotional context.

Aside from its specific relationship to maternal behavior, recent evidence more broadly implicates the BA in regulating affiliative processes such as sociability and responses to social novelty.[40,41] The basolateral amygdala (BLA) generally computes positive and negative valence signals[42] and emotional salience,[43] and it is critical for motivated behavior. Distinct subsets of BLA neurons respond to either aversive or appetitive conditioned and unconditioned stimuli.[44–47] Each subset tends to preferentially access different downstream targets.[48,49] Many BLA neurons exhibit positive (or negative) responses to

multiple positive (or negative) stimuli, suggesting that they encode valence independent of the specific stimulus.[50] Less is known about activity in the basomedial amygdala, but it may be more closely linked to controlling behavioral aversion.[51,52] Finally, analysis of ensembles embedded in a large population of simultaneously recorded BA neurons across diverse behavioral conditions shows that these ensembles adopt distinct network configurations to encode long-term behavioral states such as social or spatial exploration.[53,54]

It is not known what computed quantities are represented by BA neurons that project to the AC, but all of the above observations reveal characteristics that they may share with other BA neurons. In any case, BA-AC neurons seem unlikely to carry straightforward sensory responses to odors. Given the known properties of the BA, they likely represent more abstract affective or state variables. We propose that the direct modulation of primary sensory activity with respect to these variables constitutes an underappreciated function of the amygdala.

Future work

This work raises several interesting questions for future study. First, how are the population signals we detect here distributed among individual BA-AC neurons? Do they share the reported properties of other BA neurons? Recording from or imaging many identified individual neurons simultaneously during maternal behavior could help answer those questions. Second, are there state changes during maternal behavior such as arousal or engagement that could be in part modulated by the BA, affecting the responses to vocal signals? Future experiments might therefore focus on large-scale network dynamics in AC during maternal interactions and how they are altered by inputs from BA. Third, what aspects of maternal encounters are shared with other targets of BA, including reward circuits in the ventral pallidum and NAcc, and what effect do they have there?

RESOURCE AVAILABILITY

Lead contact

Further information and requests for resources and reagents should be directed to and will be fulfilled by the lead contact, Stephen D. Shea (sshea@cshl.edu).

Materials availability

This study did not generate new unique reagents.

Data and code availability

- All data reported in this paper will be shared by the lead contact upon request.
- This paper does not report original code.
- Any additional information required to reanalyze the data reported in this paper is available from the lead contact upon request.

ACKNOWLEDGMENTS

The authors wish to thank J. Sturgill for technical assistance; the Zador, Tollkuhn, and Li laboratories for their contributions; and Shea Lab members for helpful comments and discussion. Figures 1A, 1B, 3A, 3B, and 6A were created using Biorender.com. This work was supported by a grant to SDS from the National Institute of Mental Health (R01MH119250) and a grant to SDS from the C.M. Robertson Foundation.

AUTHOR CONTRIBUTIONS

Conceptualization, S.D.S. and A.C.N.; methodology, A.C.N., C.K., and S.D.S.; software: C.K. and S.D.S.; formal analysis, A.C.N. and S.D.S.; investigation: A.C.N., J.C., and H.T.; writing – original draft: A.C.N. and S.D.S.; writing – review and editing: all authors; visualization, A.C.N. and S.D.S.; supervision and funding acquisition, S.D.S.

DECLARATION OF INTERESTS

The authors declare no competing interests.

STAR★METHODS

Detailed methods are provided in the online version of this paper and include the following:

- KEY RESOURCES TABLE
- EXPERIMENTAL MODEL AND STUDY PARTICIPANTS DETAILS
  - Animals
- METHOD DETAILS
  - Retrieval behavior
  - MOE ablation
  - Surgical procedures
  - Fiber photometry
  - Odor presentation
  - USV recording and playback
  - Electrophysiology
  - Optogenetic stimulation
  - Post-mortem histology and immunohistochemistry
- QUANTIFICATION AND STATISTICAL ANALYSIS

SUPPLEMENTAL INFORMATION

Supplemental information can be found online at https://doi.org/10.1016/j.cub.2024.10.078.

Received: March 26, 2024
Revised: October 3, 2024
Accepted: October 30, 2024
Published: November 27, 2024

REFERENCES

1. Miranda, J.A., and Liu, R.C. (2009). Dissecting natural sensory plasticity: hormones and experience in a maternal context. Hear. Res. *252*, 21–28. https://doi.org/10.1016/j.heares.2009.04.014.
2. Ehret, G., Koch, M., Haack, B., and Markl, H. (1987). Sex and parental experience determine the onset of an instinctive behavior in mice. Naturwissenschaften *74*, 47.
3. Stolzenberg, D.S., and Champagne, F.A. (2016). Hormonal and non-hormonal bases of maternal behavior: The role of experience and epigenetic mechanisms. Horm. Behav. *77*, 204–210. https://doi.org/10.1016/j.yhbeh.2015.07.005.
4. Rosenblatt, J.S. (1967). Nonhormonal basis of maternal behavior in the rat. Science *156*, 1512–1514. https://doi.org/10.1126/science.156.3781.1512.
5. Lau, B.Y.B., Krishnan, K., Huang, Z.J., and Shea, S.D. (2020). Maternal experience-dependent cortical plasticity in mice is circuit- and stimulus-specific and requires MECP2. J. Neurosci. *40*, 1514–1526. https://doi.org/10.1523/JNEUROSCI.1964-19.2019.
6. Krishnan, K., Lau, B.Y.B., Ewall, G., Huang, Z.J., and Shea, S.D. (2017). MECP2 regulates cortical plasticity underlying a learned behaviour in adult female mice. Nat. Commun. *8*, 14077. https://doi.org/10.1038/ncomms14077.

7. Galindo-Leon, E.E., Lin, F.G., and Liu, R.C. (2009). Inhibitory plasticity in a lateral band improves cortical detection of natural vocalizations. Neuron *62*, 705–716. https://doi.org/10.1016/j.neuron.2009.05.001.

8. Cohen, L., Rothschild, G., and Mizrahi, A. (2011). Multisensory integration of natural odors and sounds in the auditory cortex. Neuron *72*, 357–369. https://doi.org/10.1016/j.neuron.2011.08.019.

9. Cohen, L., and Mizrahi, A. (2015). Plasticity during motherhood: changes in excitatory and inhibitory layer 2/3 neurons in auditory cortex. J. Neurosci. *35*, 1806–1815. https://doi.org/10.1523/JNEUROSCI.1786-14.2015.

10. Carcea, I., Caraballo, N.L., Marlin, B.J., Ooyama, R., Riceberg, J.S., Mendoza Navarro, J.M., Opendak, M., Diaz, V.E., Schuster, L., Alvarado Torres, M.I., et al. (2021). Oxytocin neurons enable social transmission of maternal behaviour. Nature *596*, 553–557. https://doi.org/10.1038/s41586-021-03814-7.

11. Weiss, J., Pyrski, M., Jacobi, E., Bufe, B., Willnecker, V., Schick, B., Zizzari, P., Gossage, S.J., Greer, C.A., Leinders-Zufall, T., et al. (2011). Loss-of-function mutations in sodium channel Nav1.7 cause anosmia. Nature *472*, 186–190. https://doi.org/10.1038/nature09975.

12. Wang, Z., and Storm, D.R. (2011). Maternal behavior is impaired in female mice lacking type 3 adenylyl cyclase. Neuropsychopharmacology *36*, 772–781. https://doi.org/10.1038/npp.2010.211.

13. Fraser, E.J., and Shah, N.M. (2014). Complex chemosensory control of female reproductive behaviors. PLoS One *9*, e90368. https://doi.org/10.1371/journal.pone.0090368.

14. Okabe, S., Nagasawa, M., Kihara, T., Kato, M., Harada, T., Koshida, N., Mogi, K., and Kikusui, T. (2013). Pup odor and ultrasonic vocalizations synergistically stimulate maternal attention in mice. Behav. Neurosci. *127*, 432–438. https://doi.org/10.1037/a0032395.

15. Petrovich, G.D., Risold, P.Y., and Swanson, L.W. (1996). Organization of projections from the basomedial nucleus of the amygdala: a PHAL study in the rat. J. Comp. Neurol. *374*, 387–420. https://doi.org/10.1002/(SICI)1096-9861(19961021)374:3<387::AID-CNE6>3.0.CO;2-Y.

16. Perry, C.J., and McNally, G.P. (2013). A role for the ventral pallidum in context-induced and primed reinstatement of alcohol seeking. Eur. J. Neurosci. *38*, 2762–2773. https://doi.org/10.1111/ejn.12283.

17. Numan, M., Bress, J.A., Ranker, L.R., Gary, A.J., Denicola, A.L., Bettis, J.K., and Knapp, S.E. (2010). The importance of the basolateral/basomedial amygdala for goal-directed maternal responses in postpartum rats. Behav. Brain Res. *214*, 368–376. https://doi.org/10.1016/j.bbr.2010.06.006.

18. Canteras, N.S., Simerly, R.B., and Swanson, L.W. (1995). Organization of projections from the medial nucleus of the amygdala: a PHAL study in the rat. J. Comp. Neurol. *360*, 213–245. https://doi.org/10.1002/cne.903600203.

19. Pereira, T.D., Tabris, N., Matsliah, A., Turner, D.M., Li, J., Ravindranath, S., Papadoyannis, E.S., Normand, E., Deutsch, D.S., Wang, Z.Y., et al. (2022). SLEAP: A deep learning system for multi-animal pose tracking. Nat. Methods *19*, 486–495. https://doi.org/10.1038/s41592-022-01426-1.

20. Cazakoff, B.N., Lau, B.Y.B., Crump, K.L., Demmer, H.S., and Shea, S.D. (2014). Broadly tuned and respiration-independent inhibition in the olfactory bulb of awake mice. Nat. Neurosci. *17*, 569–576. https://doi.org/10.1038/nn.3669.

21. Saravanan, V., Berman, G.J., and Sober, S.J. (2020). Application of the hierarchical bootstrap to multi-level data in neuroscience. Neuron Behav Data Anal Theory *3*.

22. Ehret, G., and Haack, B. (1981). Categorical perception of mouse pup ultrasound by lactating females. Naturwissenschaften *68*, 208–209.

23. Hernandez-Miranda, L.R., Ruffault, P.L., Bouvier, J.C., Murray, A.J., Morin-Surun, M.P., Zampieri, N., Cholewa-Waclaw, J.B., Ey, E., Brunet, J.F., Champagnat, J., et al. (2017). Genetic identification of a hindbrain nucleus essential for innate vocalization. Proc. Natl. Acad. Sci. USA *114*, 8095–8100. https://doi.org/10.1073/pnas.1702893114.

24. Rupert, D.D., Pagliaro, A., Choe, J., and Shea, S.D. (2023). Selective deletion of Methyl CpG binding protein 2 from parvalbumin interneurons in the auditory cortex delays the onset of maternal retrieval in mice. J. Neurosci. *43*, 6745–6759.

25. Tsuneoka, Y., Yoshihara, C., Ohnishi, R., Yoshida, S., Miyazawa, E., Yamada, M., Horiguchi, K., Young, W.S., Nishimori, K., Kato, T., and Kuroda, K.O. (2022). Oxytocin Facilitates Allomaternal Behavior under Stress in Laboratory Mice. eNeuro *9*, ENEURO.0405-21.2022. https://doi.org/10.1523/ENEURO.0405-21.2022.

26. Pi, H.J., Hangya, B., Kvitsiani, D., Sanders, J.I., Huang, Z.J., and Kepecs, A. (2013). Cortical interneurons that specialize in disinhibitory control. Nature *503*, 521–524. https://doi.org/10.1038/nature12676.

27. Grosso, A., Cambiaghi, M., Renna, A., Milano, L., Roberto Merlo, G., Sacco, T., and Sacchetti, B. (2015). The higher order auditory cortex is involved in the assignment of affective value to sensory stimuli. Nat. Commun. *6*, 8886. https://doi.org/10.1038/ncomms9886.

28. David, S.V., Fritz, J.B., and Shamma, S.A. (2012). Task reward structure shapes rapid receptive field plasticity in auditory cortex. Proc. Natl. Acad. Sci. USA *109*, 2144–2149. https://doi.org/10.1073/pnas.1117717109.

29. Concina, G., Renna, A., Grosso, A., and Sacchetti, B. (2019). The auditory cortex and the emotional valence of sounds. Neurosci. Biobehav. Rev. *98*, 256–264. https://doi.org/10.1016/j.neubiorev.2019.01.018.

30. Chavez, C.M., McGaugh, J.L., and Weinberger, N.M. (2013). Activation of the basolateral amygdala induces long-term enhancement of specific memory representations in the cerebral cortex. Neurobiol. Learn. Mem. *101*, 8–18. https://doi.org/10.1016/j.nlm.2012.12.013.

31. Chavez, C.M., McGaugh, J.L., and Weinberger, N.M. (2009). The basolateral amygdala modulates specific sensory memory representations in the cerebral cortex. Neurobiol. Learn. Mem. *91*, 382–392. https://doi.org/10.1016/j.nlm.2008.10.010.

32. Yang, Y., Liu, D.Q., Huang, W., Deng, J., Sun, Y., Zuo, Y., and Poo, M.M. (2016). Selective synaptic remodeling of amygdalocortical connections associated with fear memory. Nat. Neurosci. *19*, 1348–1355. https://doi.org/10.1038/nn.4370.

33. Yoles-Frenkel, M., Shea, S.D., Davison, I.G., and Ben-Shaul, Y. (2022). The Bruce effect: Representational stability and memory formation in the accessory olfactory bulb of the female mouse. Cell Rep. *40*, 111262. https://doi.org/10.1016/j.celrep.2022.111262.

34. Shea, S.D., Katz, L.C., and Mooney, R. (2008). Noradrenergic induction of odor-specific neural habituation and olfactory memories. J. Neurosci. *28*, 10711–10719. https://doi.org/10.1523/JNEUROSCI.3853-08.2008.

35. Kilgard, M.P., and Merzenich, M.M. (1998). Plasticity of temporal information processing in the primary auditory cortex. Nat. Neurosci. *1*, 727–731.

36. Froemke, R.C., Merzenich, M.M., and Schreiner, C.E. (2007). A synaptic memory trace for cortical receptive field plasticity. Nature *450*, 425–429. https://doi.org/10.1038/nature06289.

37. Bakin, J.S., and Weinberger, N.M. (1996). Induction of a physiological memory in the cerebral cortex by stimulation of the nucleus basalis. Proc. Natl. Acad. Sci. USA *93*, 11219–11224.

38. Numan, M., and Young, L.J. (2016). Neural mechanisms of mother-infant bonding and pair bonding: Similarities, differences, and broader implications. Horm. Behav. *77*, 98–112. https://doi.org/10.1016/j.yhbeh.2015.05.015.

39. Numan, M., Stolzenberg, D.S., Dellevigne, A.A., Correnti, C.M., and Numan, M.J. (2009). Temporary inactivation of ventral tegmental area neurons with either muscimol or baclofen reversibly disrupts maternal behavior in rats through different underlying mechanisms. Behav. Neurosci. *123*, 740–751. https://doi.org/10.1037/a0016204.

40. Mesquita, L.T., Abreu, A.R., de Abreu, A.R., de Souza, A.A., de Noronha, S.R., Silva, F.C., Campos, G.S.V., Chianca, D.A., Jr., and de Menezes, R.C. (2016). New insights on amygdala: Basomedial amygdala regulates the physiological response to social novelty. Neuroscience *330*, 181–190. https://doi.org/10.1016/j.neuroscience.2016.05.053.

41. Huang, W.C., Zucca, A., Levy, J., and Page, D.T. (2020). Social Behavior Is Modulated by Valence-Encoding mPFC-Amygdala Sub-circuitry. Cell Rep. *32*, 107899. https://doi.org/10.1016/j.celrep.2020.107899.

42. O'Neill, P.K., Gore, F., and Salzman, C.D. (2018). Basolateral amygdala circuitry in positive and negative valence. Curr. Opin. Neurobiol. *49*, 175–183. https://doi.org/10.1016/j.conb.2018.02.012.

43. SenGupta, A., Yau, J.O.Y., Jean-Richard-dit-Bressel, P., Liu, Y., Millan, E.Z., Power, J.M., and McNally, G.P. (2018). Basolateral Amygdala Neurons Maintain Aversive Emotional Salience. J. Neurosci. *38*, 3001–3012. https://doi.org/10.1523/JNEUROSCI.2460-17.2017.

44. Paton, J.J., Belova, M.A., Morrison, S.E., and Salzman, C.D. (2006). The primate amygdala represents the positive and negative value of visual stimuli during learning. Nature *439*, 865–870. https://doi.org/10.1038/nature04490.

45. Beyeler, A., Chang, C.J., Silvestre, M., Lévêque, C., Namburi, P., Wildes, C.P., and Tye, K.M. (2018). Organization of Valence-Encoding and Projection-Defined Neurons in the Basolateral Amygdala. Cell Rep. *22*, 905–918. https://doi.org/10.1016/j.celrep.2017.12.097.

46. Belova, M.A., Paton, J.J., and Salzman, C.D. (2008). Moment-to-moment tracking of state value in the amygdala. J. Neurosci. *28*, 10023–10030. https://doi.org/10.1523/JNEUROSCI.1400-08.2008.

47. Belova, M.A., Paton, J.J., Morrison, S.E., and Salzman, C.D. (2007). Expectation modulates neural responses to pleasant and aversive stimuli in primate amygdala. Neuron *55*, 970–984. https://doi.org/10.1016/j.neuron.2007.08.004.

48. Senn, V., Wolff, S.B.E., Herry, C., Grenier, F., Ehrlich, I., Gründemann, J., Fadok, J.P., Müller, C., Letzkus, J.J., and Lüthi, A. (2014). Long-range connectivity defines behavioral specificity of amygdala neurons. Neuron *81*, 428–437. https://doi.org/10.1016/j.neuron.2013.11.006.

49. Namburi, P., Beyeler, A., Yorozu, S., Calhoon, G.G., Halbert, S.A., Wichmann, R., Holden, S.S., Mertens, K.L., Anahtar, M., Felix-Ortiz, A.C., et al. (2015). A circuit mechanism for differentiating positive and negative associations. Nature *520*, 675–678. https://doi.org/10.1038/nature14366.

50. Gore, F., Schwartz, E.C., Brangers, B.C., Aladi, S., Stujenske, J.M., Likhtik, E., Russo, M.J., Gordon, J.A., Salzman, C.D., and Axel, R. (2015). Neural Representations of Unconditioned Stimuli in Basolateral Amygdala Mediate Innate and Learned Responses. Cell *162*, 134–145. https://doi.org/10.1016/j.cell.2015.06.027.

51. Ineichen, C., Greter, A., Baer, M., Sigrist, H., Sautter, E., Sych, Y., Helmchen, F., and Pryce, C.R. (2022). Basomedial amygdala activity in mice reflects specific and general aversion uncontrollability. Eur. J. Neurosci. *55*, 2435–2454. https://doi.org/10.1111/ejn.15090.

52. Adhikari, A., Lerner, T.N., Finkelstein, J., Pak, S., Jennings, J.H., Davidson, T.J., Ferenczi, E., Gunaydin, L.A., Mirzabekov, J.J., Ye, L., et al. (2015). Basomedial amygdala mediates top-down control of anxiety and fear. Nature *527*, 179–185. https://doi.org/10.1038/nature15698.

53. Gründemann, J., Bitterman, Y., Lu, T., Krabbe, S., Grewe, B.F., Schnitzer, M.J., and Lüthi, A. (2019). Amygdala ensembles encode behavioral states. Science *364*, eaav8736. https://doi.org/10.1126/science.aav8736.

54. Fustiñana, M.S., Eichlisberger, T., Bouwmeester, T., Bitterman, Y., and Lüthi, A. (2021). State-dependent encoding of exploratory behaviour in the amygdala. Nature *592*, 267–271. https://doi.org/10.1038/s41586-021-03301-z.

55. Marinez-Cagigal, V. (2018). ROC Curve. https://www.mathworks.com/matlabcentral/fileexchange/52442-roc-curve.

56. Friard, O., and Gamba, M. (2016). BORIS: A free, versatile open-source event-logging software for video/audio coding and live observations. Methods Ecol. Evol. *7*, 1325–1330.

57. Millan, E.Z., Kim, H.A., and Janak, P.H. (2017). Optogenetic activation of amygdala projections to nucleus accumbens can arrest conditioned and unconditioned alcohol consummatory behavior. Neuroscience *360*, 106–117. https://doi.org/10.1016/j.neuroscience.2017.07.044.

58. Kim, J., Zhang, X., Muralidhar, S., LeBlanc, S.A., and Tonegawa, S. (2017). Basolateral to Central Amygdala Neural Circuits for Appetitive Behaviors. Neuron *93*, 1464–1479.e5. https://doi.org/10.1016/j.neuron.2017.02.034.

59. Yizhar, O., Fenno, L.E., Davidson, T.J., Mogri, M., and Deisseroth, K. (2011). Optogenetics in neural systems. Neuron *71*, 9–34. https://doi.org/10.1016/j.neuron.2011.06.004.

60. Dunston, D., Ashby, S., Krosnowski, K., Ogura, T., and Lin, W. (2013). An effective manual deboning method to prepare intact mouse nasal tissue with preserved anatomical organization. J. Vis. Exp. *10*, 50538. https://doi.org/10.3791/50538.

STAR★METHODS

KEY RESOURCES TABLE

REAGENT or RESOURCE	SOURCE	IDENTIFIER
Antibodies		
Chicken Anti-GFP	AVES	GFP-1020; RRID: AB_10000240
Goat anti-chicken Alexa 488	Invitrogen	A-11039; RRID: AB_2534096
Bacterial and virus strains		
AAVrg.CAG.tdTomato	Addgene	59462-AAVrg
AAVrg.pmSyn1.EBFP.Cre	Addgene	5107-AAVrg
AAVrg.hSyn.Cre.WPRE.hGH	Addgene	105553-AAVrg
AAVrg.FLEX.tdTomato	Addgene	28306-AAVrg
AAV5.syn.FLEX.GCaMP6s.WPRE	Addgene	100845-AAV5
AAV9.synP.DIO.EGFP.WPRE.hGH	Addgene	100043-AAV9
AAV9.CAGGS.Flex.ChR2.tdTomato.WPRE.SV40	UPenn Viral Core	N/A
Chemicals, peptides, and recombinant proteins		
Mineral Oil	Sigma	330779
Amyl Acetate	Sigma	W504009
Ethyl Tiglate	Sigma	W246000
R-Carvone	Sigma	124931
S-Carvone	Sigma	435759
Experimental models: Organisms/strains		
CBA/CaJ	The Jackson Laboratory	000654
H2B-GFP (Rosa26-stopflox-H2B-GFP)	Bo Li Lab, generated by Josh Huang	N/A
VGlut1Cre (Slc17a7tm1.1(cre)Hze/J	The Jackson Laboratory	023527
VGlut2Cre (Slc17a6tm2(cre)Lowl/J	The Jackson Laboratory	016963
VGatCre (Slc32a1tm2(cre)Lowl/J	The Jackson Laboratory	016962
Software and algorithms		
MATLAB 2023b	Mathworks	https://www.mathworks.com/products/matlab.html
Python 3.10.14	Python Software Foundation	https://www.python.org
SLEAP	Pereira et al.[19]	https://sleap.ai/
ROC Curve	Marinez-Cagigal[55] MATLAB Central File Exchange	https://www.mathworks.com/matlabcentral/fileexchange/52442-roc-curve
Spike2	CED	https://ced.co.uk/products/spkovin
Prism	GraphPad	https://www.graphpad.com/features
FIJI	fiji.sc	N/A
Other		
Bed'r Nest nesting material	Lab Supply	N/A
–	–	https://imagej.net/software/fiji/
–	Lab Supply	BRN

EXPERIMENTAL MODEL AND STUDY PARTICIPANTS DETAILS

Animals

All procedures were conducted in accordance with the National Institutes of Health's Guide for the Care and Use of Laboratory Animals and approved by the Cold Spring Harbor Laboratory Institutional Animal Care and Use Committee. All experiments were performed on adult (aged 6-12 weeks) female mice that were maintained on a 12h:12h light-dark cycle and received food *ad libitum*. Throughout the text and figure legends, 'n' is used to refer the number of individual biological replicates. Due to the exploratory nature

of our work, we did not a priori compute sample size for any of our experiments. Most mice were CBA/CaJ (Jax #000654), however neuroanatomical tracing experiments were performed in H2B-GFP (*Rosa26-stop^{flox}-H2B-GFP*, gift from Bo Li), VGlut1Cre (*Slc17a7$^{tm1.1(cre)Hze}$/J*; Jax #023527), VGlut2Cre (*Slc17a6$^{tm2(cre)Lowl}$/J*; Jax #016963), or VGatCre (*Slc32a1$^{tm2(cre)Lowl}$/J*; Jax #016962). We performed all behavioral experiments during the dark cycle.

METHOD DETAILS

Retrieval behavior

Surrogates were generated by co-housing a virgin female with a pregnant CBA/CaJ dam beginning 1-5 days prior to birth. Pup retrieval behavior performance was first assayed on the day pups were born (P0) and again on P3 and P5 as described.[6] Briefly, retrieval behavior was performed in the home cage (39 cm by 20 cm by 16 cm), which was placed in a larger dark, sound-attenuated chamber (61 cm by 58 cm by 56 cm). The mother was removed and a surrogate was allowed to habituate to the behavior chamber in its home cage for 5 min with 5 pups in the nest. Pups were then removed for 2 minutes and subsequently returned to all four corners and the center. The trial started when the last pup was placed and each surrogate was given 5 minutes to retrieve all pups back to the nest. Videos were recorded in the dark under infrared light using a Logitech webcam (c920) with the IR filter removed.

Behavioral videos were annotated using BORIS (Behavior Observation Research Interactive Software)[56] by a trained observer who was blind to the experimental condition and day of testing. The observer manually scored the onset and offset of events including 'search', 'retrieval success', 'retrieval error', 'investigation', 'air sniff', and 'nesting', which were exported to MATLAB for further analysis. A normalized latency score was calculated using the following formula:

$$norm.\frac{\sum(t_1 - t_0), (t_2 - t_0), \ldots, (t_n - t_0),}{n \times L}$$

n = number of pups outside the nest, t_0 = start of the trial, t_n = time the nth pup was gathered, L = trial length (300s).

MOE ablation

Following five days of maternal experience, surrogates were given an intraperitoneal (IP) injection of methimazole (MMZ; 50 mg/kg) (Millipore Sigma, #46429) dissolved in saline. We waited 7 days to allow sufficient time for the MOE to degenerate before retesting mice in the retrieval assay.

Surgical procedures

Before all surgical procedures, mice were initially anesthetized with an IP injection (1.25 ml/kg) of an 80:20 mixture of ketamine (100 mg/ml) and xylazine (20 mg/ml) and were stabilized in a stereotaxic frame. Anesthesia was maintained throughout by vaporized isoflurane (1 – 2% as needed).

Depending on the specific experiment, we injected one or more adeno-associated viruses (AAVs) into the auditory cortex (45nL of virus in 6 injection sites, AP: -1.7, -2.1, -2.4mm, ML: 4.0mm, DV: -0.35, -0.55mm as measured from cortical surface) and/or the basal amygdala (200nL of virus, AP: -1.5mm, ML: 3.0mm, DV: -5.4mm), as described in results. See key resources table for specific constructs used, serotype, and ordering information. After the target volume of virus was expelled, the injection pipette was slowly retracted from the brain. In mice prepared for fiber photometry, a 5 mm length of 200 μm optical fiber (0.39 NA, Thorlabs) was implanted 200 μm above the BA injection site before being secured with Metabond dental cement along with a titanium head fixation bar. The scalp was sutured shut and the mouse was given a dose of meloxicam (2 mg/mL) for analgesia.

Fiber photometry

Experiments were performed with a custom-built two-color fiber photometry system. The output from two LEDs (470nm/565nm; Doric) was focused into a fiber launch holding a 200 μm optical fiber (0.37 NA; Doric) that could be coupled to the implanted optical fiber via a lightweight, flexible cable during daily recording sessions. The LEDs were sinusoidally modulated 180 degrees out of phase at 211 Hz and emitted green and red light was collected from the optical fiber. Each color was separated and bandpass filtered and was detected by a dedicated photoreceiver (#2151, Newport Corporation). Light delivered to the brain was measured at ~30 mW at the fiber tip.

Animals used in head-fixed recording sessions were habituated to fixation for 30-60 minutes once a day for 3-5 days prior to testing. At the start of each session, animals were connected to the patch cord and baseline signal was recorded for 2 minutes. Recordings from freely behaving mice were conducted identically with the exception that the cable attached to the head led to an optical swivel (Doric) to allow free movement. The signal from each photoreceiver was digitized at a sampling rate of 6100 Hz and acquired to a computer via a National Instruments DAQ device (NI-USB6211).

The raw data were used to calculate ΔF/F signals offline with custom written MATLAB code. First, the value at each peak in the sinusoidal signals was detected, resulting in an effective sampling rate of 211 Hz. Each signal was low pass filtered at 15 Hz and fit to a double exponential decay function, which was subtracted to correct for photobleaching during the trial. To correct for any movement artifact, we used a robust regression to compute a linear function for predicting the activity-independent component of the green signal based on the red. This component, which was in most cases small, was subtracted from the green signal. Finally, the result was mean subtracted and then divided by the mean to calculate ΔF/F. ΔF/F signals were Z-scored across all recording

sessions from each mouse to compare calcium activity from multiple animals and days. The notation 'Z-dFF' is used here to distinguish Z-score normalized ΔF/F signals from raw ΔF/F signals ('dFF').

Four mice were excluded from the study as they did not exhibit fluctuations in their Ca^{2+} signal (likely due to misalignment in fiber placement). Individual trials were excluded if the Ca^{2+} trace contained unacceptably high contamination from artifact or if retrieval behavior was obscured. No subjects or trials were excluded for any other reason.

Odor presentation

Controlled presentation of odors to awake, head-fixed mice was achieved with a custom-built olfactometer as described.[20] Briefly, mice were head-fixed to a frame with their nose positioned in front of an odor port on a 10 cm diameter foam wheel. The wheel permitted the animal to freely walk or run or remain still. To deliver monomolecular odors, clean oxygen flow was briefly redirected by a solenoid assembly through the headspace of one of eight vials containing one odor (key resources table) diluted to 5% V/V in mineral oil. The odorized oxygen was mixed (1:10) with a clean air carrier stream to achieve a flow dilution of 0.5% saturated vapor. Pup and nesting material odors were presented by placing 3 pups or clean nesting material in a sealed chamber (4 oz mason jar) and swapping it with one of the odor vials in our olfactometer. Half of the pup chamber was kept on a warm pad and pup odor trials were limited to 10 minutes per session for the pups' safety and comfort. Pups used for odor stimulation were used a maximum of 6 sessions per day and were returned to their mothers immediately following the experiment.

USV recording and playback

Single pup vocalizations and tones were presented during electrophysiology recordings using one of the output channels of a National Instruments DAQ (NI-USB 6211) controlled by custom software written in MATLAB. Output was sent to an electrostatic speaker driver powering an electrostatic speaker (ED1/ES1, Tucker-Davis Technologies) positioned 4 inches behind the animal's head. Stimuli were low pass filtered and amplified at 100kHz using a custom filter and preamp (Kiwa Electronics). A sound level meter (Model 407736, 'A' weighting; Ex-Tech) was used to calibrate the RMS for all stimuli to 70 dB SPL at the head. USVs were detected using a polarized condenser ultrasound microphone (CM16/CMPA, Avisoft Bioacoustics) placed 12'' above the cage floor and were digitally sampled at 200 kHz via a National Instruments DAQ (NI-USB 6211) using custom software written in MATLAB.

Electrophysiology

Prior to recording, the mouse was anesthetized with an 80:20 mixture (1.25ml/kg) of ketamine (100mg/ml) and xylazine (20 mg/ml). Anesthesia was maintained throughout the recording by subsequent microinjections of ketamine. Extracellular recordings were made using the 'loose patch' method.[5,20] Micropipettes were pulled from borosilicate glass filaments (O.D. 1.5mm, I.D. 0.86mm; BF150-86-10, Sutter Instrument) using a Flaming/Brown micropipette puller (P-97; Sutter Instruments) and back-filled with intracellular solution (125 mM potassium gluconate, 10mM potassium chloride, 2mM magnesium chloride, and 10mM HEPES pH 7.2) for a final resistance of 10 – 30 MΩ. Isolated single-unit neural activity was recorded using a BA-03X bridge amplifier (npi), low-pass filtered at 3 kHz, digitized at 10 kHz, and acquired using Spike2 software (v.7; Cambridge Electronic Design). Recording depth was measured by a piezoelectric micromanipulator (Sutter Instrument SOLO/E-116). All neurons were found from 300 μm – 1200 μm from the cortical surface, corresponding to approximately layers II – VI of auditory cortex.

Experiments were performed in an anechoic, sound-attenuated chamber (Industrial Acoustics). Single pup vocalizations and tones were presented to surrogates using one of the output channels on a Power1401 ADC/DAC board (Cambridge Electronic Design). Stimuli were low pass filtered at 100kHz and amplified using a custom filter and preamp (Kiwa Electronics). Output was sent to an electrostatic speaker driver powering an electrostatic speaker (ED1/ES1, Tucker-Davis Technologies) positioned 4 inches in front of the animal. All stimuli were calibrated to RMS of 65dB SPL at the animal's head using a sound level meter (Ex-Tech, model 407736). Stimuli consisted of 7 log-spaced pure tones (16, 20, 25, 32, 40, 50, 64 kHz) or 8 natural pup calls recorded from CBA/CaJ mouse pups on postnatal day 2 (calls 1-4) or 4 (calls 5-8). Stimuli were presented for 100ms at an interstimulus interval of 4s.

Optogenetic stimulation

To optogenetically activate BA terminals in the auditory cortex, the tip of an optical fiber (∅ 400 μm NA 0.39; Thor Labs) was positioned just over the craniotomy with a micromanipulator such that light shone directly on the cortical surface. Trains of light pulses were controlled by the timing output of an isolated pulse stimulator (A-M Systems) and consisted of 10 ms pulses of blue light (473nm; OEM laser) delivered at 20 Hz for 1 s[57,58] and beginning 500 ms prior to the auditory stimulus. Laser power was 30 mW as measured at the tip of the optic fiber. Based on this, we estimate the power to be 2 – 10 mW/mm^2 at a depth of 300-1000 mm from the cortical surface,[59] where most recordings were made.

Post-mortem histology and immunohistochemistry

At the end of each experiment, mice were delivered a lethal dose of pentobarbital (Euthasol), and then exsanguinated and transcardially perfused with PBS followed by 4% paraformaldehyde. In cases where the tissue was required for staining and/or microscopy, the brain and the main olfactory epithelium (MOE) were extracted and post-fixed overnight at 4°C. Brains were then transferred to a solution of 30% sucrose in PBS overnight at room temperature (RT) and subsequently sectioned on a freezing microtome at a thickness of 50μm. For visualization of GCaMP6s expression, brain sections were first incubated with a primary antibody raised against GFP in chicken (AVES) diluted 1:1000 in PDT (0.5% normal donkey serum, 0.1% Triton X-100 \in PBS) at 4 degrees overnight and then

stained with a secondary anti-chicken Alexa 488 fluorophore raised in goat and diluted 1:500 in PDT for 2 h at room temperature. Nasal tissue was dissected from the skull[60] and sent to the CSHL histology core to be paraffin sectioned, H&E stained, and compared to a saline injected control (Figure 1). MOE ablation was confirmed by manual inspection of the processed tissue.

QUANTIFICATION AND STATISTICAL ANALYSIS

All data analysis was performed with either Matlab (Mathworks) or Prism 9 software (GraphPad). Information about statistical details can be found in the figure legends. Unless otherwise noted, data are reported as mean ± standard error. Electrophysiology data were manually spike sorted into single unit spike trains with Spike2 (CED). All subsequent analyses were performed with custom-written code in MATLAB (Mathworks). Mean baseline firing rate was calculated as the mean spontaneous firing rate during a 1 s period just before each stimulus. This quantity was subtracted from the stimulus-evoked spike rate measured from 50 – 200 ms after the onset of each stimulus to calculate 'response strength.' Neurons that were presented fewer than 6 trials or had a mean firing rate of less than 0.5 spikes per trial were excluded from analysis, unless they exhibited clear auditory responses. To assess the statistical significance of responses to each auditory stimulus, we used a bootstrap procedure. For a response window length t, and a stimulus presented n times, we created a null distribution by computing the mean response strength across n windows of length t, randomly drawn from the full spike record and repeating this 10,000 times. Auditory-evoked response strengths in the top or bottom 2.5% of the null distribution were considered significantly excitatory or inhibitory auditory-evoked responses, respectively. Individual significant responses to odors in fiber photometry were similarly compared to a dummy distribution generated with a bootstrap procedure using data from the same mouse (see STAR Methods).

We used the machine learning-based markerless pose estimation tool SLEAP[19] to track the mouse's head position during freely moving behavior trials. Pythagorean distance was computed for the X-Y coordinates of the head on each pair of adjacent 30 Hz frame in the video. Neural data and speed data were each binned at 1 s and we calculated the Pearson correlation between corresponding bins. For each subject, the reported value is the mean r coefficient among multiple trials (median 11 trials per mouse).

ROC analysis was used to assess whether the distribution of auditory-evoked response strengths from light-on trials were discriminable from light-off trials for a given neuron and stimulus. Analysis was performed in MATLAB (Mathworks) using a publicly available ROC curve function.[55] Because optogenetic modulation of auditory-evoked responses could be either enhancing or suppressive, we converted all auROC values < 0.5 to 1 minus their value. These data were further analyzed using a hierarchical bootstrap procedure for multilevel data.[21] Briefly, data were resampled 1000x with replacement by mice, then by neurons, and then by stimuli to create a distribution describing the variability in estimating the mean of the population. Then we compared the distributions of surrogate and naïve mice by computing a joint probability matrix to directly quantify the percent chance of drawing overlapping samples.

To determine the degree to which optogenetic stimulation modified the firing response for each cell-stimulus pair that exhibited an auditory response, we used the following formula to calculate a modulation index. Here, RS_{aud} equals the mean response strength to a given stimulus without optogenetic stimulation, and RS_{opto}. equals the mean response strength in response to the same stimulus with optogenetic stimulation.

$$MI = \frac{RS_{aud} - RS_{apto}}{RS_{aud} + RS_{apto}}$$

Optogenetic modulation of auditory responses was categorized as either enhancing or suppressive. This classification was based on whether the mean auditory-evoked response strength during optogenetic stimulation was higher or lower than the response strength evoked by the auditory stimulus alone.

For the analysis of odor-evoked activity, we calculated the mean amplitude of the z-dFF signal over the 4 s following the onset of odor presentation, and compared that to 2 s of baseline that occurred immediately before odor onset. We also calculated the difference between the mean signal at these two time points.

To examine whether an individual cell exhibited an evoked response to light stimulation alone (without auditory stimulus), we combined data from all light-only trials collected from a single cell. We then calculated the mean response strength within the 1s window of light stimulation and assessed whether the cell exhibited a statistically significant response based on the bootstrap procedure described earlier.